Multidimensional stability of martensite twins under regular kinetics

Ramón G. Plaza*

Departamento de Matemáticas y Mecánica, IIMAS-UNAM, Apdo. Postal 20-726, C.P. 01000 México, D.F., México

Received 16 March 2007; received in revised form 19 October 2007; accepted 7 November 2007

Abstract

This paper considers phase boundaries governed by regular kinetic relations as first proposed by Abeyaratne and Knowles [1990. On the driving traction acting on a surface of strain discontinuity in a continuum. J. Mech. Phys. Solids 38 (3), 345–360; 1991. Kinetic relations and the propagation of phase boundaries in solids. Arch. Ration. Mech. Anal. 114, 119–154]. It shows that static configurations of hyperelastic materials, in which two different martensitic (monoclinic) states meet along a planar interface, are dynamically stable towards fully three-dimensional perturbations. For that purpose, the reduced stability (or reduced Lopatinski) function associated to the static twin [Freistühler and Plaza, 2007. Normal modes and nonlinear stability behavior of dynamic phase boundaries in elastic materials. Arch. Ration. Mech. Anal. 186 (1), 1–24] is computed numerically. The results show that the interface is weakly stable under Maxwellian kinetics expressing conservation of energy across the boundary, whereas it is uniformly stable with respect to linearly dissipative kinetic rules of Abeyaratne and Knowles type.
© 2007 Elsevier Ltd. All rights reserved.

MSC: 74N20; 74A50; 35L67

Keywords: Martensite twin; Multidimensional stability; Kinetic relations; Lopatinski function; Static phase boundary

1. Introduction

At appropriate temperatures, certain crystalline materials are characterized by a multiplicity of preferred *martensitic states* of deformation. Nonlinear elasticity theory (Ball and James, 1987, 1992) models such materials by a stored-energy density

$$W : \mathbb{R}^{3\times3}_+ \longrightarrow [0, +\infty) \tag{1}$$

which, as a frame-indifferent function of the deformation gradient $\mathbf{F} \in \mathbb{R}^{3\times3}_+$, has a non-convex, multiple well structure with several global minima. Being any of these minima a martensitic deformation state, each corresponding well is called a *martensitic phase*. Many such materials allow for pairs $(\underline{\mathbf{F}}^-, \underline{\mathbf{F}}^+)$ of energy

---

*Tel.: + 52 55 5622 3567; fax: + 52 55 5622 3564.

E-mail addresses: plaza@mym.iimas.unam.mx, rgplaza@gmail.com (R.G. Plaza).

minimizing martensitic states which satisfy the *Hadamard condition*,

$$\underline{\mathbf{F}}^+ - \underline{\mathbf{F}}^- = \mathbf{a} \otimes \mathbf{v} \tag{2}$$

for some $\mathbf{a}, \mathbf{v} \in \mathbb{R}^3$, $\mathbf{a} \neq 0, |\mathbf{v}| = 1$. In this case, $\underline{\mathbf{F}}^-$ and $\underline{\mathbf{F}}^+$ are called *rank-one connected*. Hadamard condition implies the existence of a continuous deformation with planar interface separating layers in which the deformation gradient is either $\underline{\mathbf{F}}^+$ or $\underline{\mathbf{F}}^-$ at each side of the plane. Such a configuration,

$$\mathbf{F}_0(x) = \begin{cases} \underline{\mathbf{F}}^-, & x \cdot \mathbf{v} < 0, \\ \underline{\mathbf{F}}^+, & x \cdot \mathbf{v} > 0, \end{cases} \quad x \in \mathbb{R}^3, \tag{3}$$

is called a *martensite twin*.

Let us identify the elastic body at rest with its reference configuration $\Omega \subset \mathbb{R}^3$. Mathematically, the function

$$(\mathbf{F}_*, \mathbf{v}_*)(x, t) := (\mathbf{F}_0(x), 0), \quad (x, t) \in \Omega \times [0, +\infty],$$

is a time-independent (static) weak solution to the equations of non-thermal elastodynamics in the absence of external forces,

$$\mathbf{F}_t - \nabla_x \mathbf{v} = 0,$$
$$\mathbf{v}_t - \mathrm{div}_x \sigma(\mathbf{F}) = 0, \tag{4}$$

together with the constraint

$$\mathrm{curl}_x \mathbf{F} = 0. \tag{5}$$

Here, $\sigma(\mathbf{F})$ denotes the (first) Piola–Kirchhoff stress tensor

$$\sigma = \frac{\partial W}{\partial \mathbf{F}},$$

and the spatial and temporal derivatives of the local deformation $\mathbf{X} : \Omega \times [0, +\infty) \to \mathbb{R}^3$,

$$\mathbf{F}(x, t) = \nabla_x \mathbf{X} \in \mathbb{R}^{3 \times 3} \quad \text{and} \quad \mathbf{v}(x, t) = \mathbf{X}_t \in \mathbb{R}^3 \tag{6}$$

(defined component-wise by,

$$\mathbf{F}_{ij} = \frac{\partial \mathbf{X}_i}{\partial x_j} \quad \text{and} \quad \mathbf{v}_i = \frac{\partial \mathbf{X}_i}{\partial t},$$

for all $i, j = 1, 2, 3$), denote the possibly time-dependent deformation gradient and local velocity, respectively, of the elastic material.

The system of equations (4) accounts for the basic balance laws of continuum mechanics (see, e.g., Dafermos, 2005), assuming that no thermal effects play a role, and that the forces within the medium derive from the energy density function W. The curl-free constraint (5) is a short-cut for the compatibility equations

$$\partial_{x_k} \mathbf{F}_{ij} - \partial_{x_j} \mathbf{F}_{ik} = 0, \quad i, j, k = 1, 2, 3,$$

which are clearly a consequence of Eqs. (6).

This paper addresses the stability of martensite twins under the viewpoint of continuum elastodynamics. More precisely, given a multidimensional smooth perturbation (or a small wave impinging on the interface) of the piecewise smooth initial data (3), is there a local solution to Eqs. (4) with the same wave pattern? In other words, will solutions $(\mathbf{F}, \mathbf{v})$ to the dynamic system of equations, whose initial data $(\mathbf{F}, \mathbf{v})(x, 0)$ are only near to—but not identical with—$(\mathbf{F}_0(x), 0)$, be close and similar to—or far and qualitatively different from—$(\mathbf{F}_*, \mathbf{v}_*)$? Considering Eq. (3) as a localized planar sharp interface, we are then concerned with the well-posedness of the associated Cauchy problem for Eqs. (4) with piecewise smooth initial data (3).

Localized traveling discontinuities arise naturally as piecewise smooth solutions to Eqs. (4), and must satisfy canonical jump conditions of Rankine–Hugoniot type expressing conservation across the interface. They are called *shocks* when they separate states in the same martensitic phase, and *phase boundaries* when the states on either side are in different phases. Martensite twins like Eq. (3) are static examples of the latter. Due to non-convexity of the stored energy W, the system of conservation laws is of mixed-type, that is, the system changes

from hyperbolic to elliptic in some regions of space. Phase boundaries, then, connect two states belonging to two different connected components of the hyperbolic region, and travel at *subsonic* speeds smaller than the local wave speeds obtained via linearization of the equations around the states at both sides of the interface.

Dynamic problems involving elastic phase boundaries are highly non-unique (Ericksen, 1975). In contrast to shocks, the propagation speed of phase boundaries cannot be completely determined by the constitutive law and momentum balance (James, 1980). As a result, an additional criterion is needed to determine the dynamics of the traveling discontinuity. There is no consensus, however, about its form. In most theories, it is usually prescribed as a constitutive *kinetic relation* which, in the simplest scenario, relates the normal velocity of the discontinuity with the driving force across the interface (Abeyaratne and Knowles, 1990, 1991). The kinetic relation induces an additional jump condition or *kinetic rule* which, just like the Rankine–Hugoniot jump conditions, interrelates the two states on either side of the boundary with its space normal and velocity.

Thanks to the fundamental work of Majda (1983a,b) and Métivier (1990), it is now known that the nonlinear stability of such traveling fronts is determined by the Lopatinski conditions of linear hyperbolic problems (Kreiss, 1970). We briefly describe the main ideas of Majda's method. Prescribing a multi-dimensional perturbation of the planar front leads to a free-boundary transmission problem, where the transmission equations are the Rankine–Hugoniot conditions (and, in the case of phase boundaries, the kinetic jump condition as well). Introducing the equation of the shock as an extra unknown, and after a shock-localization procedure (a change of coordinates permitted by the finite propagation speed), one changes the transmission problem into an *initial boundary value problem* (IBVP) in a half space. A linearization of the transformed system about the shock yields a linear hyperbolic IBVP with constant coefficients, just like the problems originally studied in the classical work of Kreiss (1970). Majda defined uniform stability of the shock front as L^2 strong well-posedness of the constant coefficients IBVP, leading to the *uniform Lopatinski condition* of Kreiss (see Majda, 1983a). To arrive at such condition one does a plane-wave analysis of the linearized problem. Thus, the starting point is the Fourier decomposition in normal modes of the constant coefficients linearized system. Majda then shows that the linearized uniform stability condition implies nonlinear stability, that is, well-posedness of the Cauchy problem associated to the full nonlinear equations, by mean of a Newton type iteration scheme (Majda, 1983a). The local-in-time existence of multidimensional shock waves also depends on the uniform stability condition (Majda, 1983b). Majda's work was later refined by Métivier (1990) using paradifferential calculus techniques and taking into account the weak (small-amplitude) limit.

Therefore, their analyses reduce the nonlinear stability of classical (Laxian) shock waves (Lax, 1957) to the verification of the uniform Lopatinski condition. Subsonic phase boundaries can be associated, in turn, to non-classical shocks of *undercompressive* type (Freistühler, 1995). It was Freistühler (1998) who first recognized the necessity to incorporate the kinetic jump condition into Majda's plane-wave analysis. Under Freistühler's suggested strategy, the Majda–Métivier theory was later extended by Coulombel (2003), who showed that the uniform Lopatinski condition implies nonlinear stability of undercompressive shocks, and subsonic phase boundaries in continuum mechanics fit into this setting. For example, the uniform Lopatinski condition for moving phase boundaries in the case of two-phase fluid flow has been extensively studied by Benzoni-Gavage (1998, 1999). Recently, Freistühler and Plaza (2007) have shown that for the equations of hyperelasticity, one can perform the plane-wave analysis needed to arrive at the stability conditions in a reduced space of amplitudes which are compatible with the curl-free constraint (5), leading to the definition of the *reduced* Lopatinski function which controls the nonlinear stability behaviour of the interface. Technically (and physically!) their reduction allows us to incorporate static phase boundaries into the analysis.

This paper is devoted to study the stability condition (and consequently, to the nonlinear dynamic stability behaviour) pertaining to a particular physical example of a static martensite twin. We have chosen an energy density modelling orthorhombic-to-monoclinic transformations (Kružík and Luskin, 2003), and the static planar interface twins two monoclinic martensitic phases (Ball and James, 1992). The definition and calculation of the associated stability function depends crucially on the choice of kinetic relation that rules the dynamics of the front and of its multidimensional perturbations. The current work considers regular kinetic relations in their simplest form, as first proposed by Abeyaratne and Knowles (1990, 1991).

In the remainder of the introduction, we describe elastic subsonic phase boundaries and their governing kinetic relations; define the Lopatinski conditions of multidimensional stability theory; and specify the form of the particular material we have chosen. Section 2 contains needed properties of the energy density and of the

kinetic rules. In Section 3 we define precisely the stability (or reduced Lopatinski) function for a martensite twin and make some simplifications which help greatly in its evaluation. Section 4 describes how to numerically compute the stability function: we describe the numerical procedure and the key ideas which allow to conclude stability. Section 5 contains the output of our computations and the stability results for the particular elastic material under consideration. We briefly discuss, in Section 6, the limitations and possible extensions of the present study.

Notation: In this paper, $\mathbb{R}^{3\times 3}_+$ denotes the set of all 3×3 matrices of positive determinant, with identity $\mathbf{I} \in \mathbb{R}^{3\times 3}_+$. With respect to the canonical (column) basis $\{\hat{e}_j\}_{j=1}^3$ of $\mathbb{R}^3$, the Piola–Kirchhoff stress tensor $\sigma(\mathbf{F})$ has (i,j)-component $\sigma_{ij}(\mathbf{F}) = \partial W/\partial \mathbf{F}_{ij}$, for $1 \leqslant i,j \leqslant 3$. $\mathbf{F}_j$ and σ_j denote the jth column of $\mathbf{F}$ and σ, respectively. To express the second derivatives of the energy, for each pair (i,j), we define the 3×3 matrix fields $\mathbf{B}_i^j(\mathbf{F}) = \partial \sigma_j/\partial \mathbf{F}_i$, whose (l,k)-entry[1] is

$$(\mathbf{B}_i^j(\mathbf{F}))_{lk} = \frac{\partial^2 W}{\partial \mathbf{F}_{lj} \partial \mathbf{F}_{ki}}.$$

The $\mathbf{B}_i^j$ are mutual transposes, $(\mathbf{B}_i^j)^\top = \mathbf{B}_j^i$, $1 \leqslant i,j \leqslant 3$, and define the acoustic tensor as

$$\mathbf{N}(\xi,\mathbf{F}) = \sum_{i,j=1}^3 \xi_i \xi_j \mathbf{B}_i^j(\mathbf{F}), \tag{7}$$

for all $\mathbf{F} \in \mathbb{R}^{3\times 3}$ and $\xi \in \mathbb{R}^3$. When evaluating at the wells (22), we write $\mathbf{B}_i^{j\pm} := \mathbf{B}_i^j(\underline{\mathbf{F}}^\pm)$ and $\mathbf{C}^\pm := (\underline{\mathbf{F}}^\pm)^\top \underline{\mathbf{F}}^\pm$. Eqs. (4) constitute a system of conservation laws of form

$$u_t + \sum_j f_j(u)_{x_j} = 0,$$

with state variables and fluxes

$$u = \begin{pmatrix} \mathbf{F}_1 \\ \mathbf{F}_2 \\ \mathbf{F}_3 \\ \mathbf{v} \end{pmatrix} \in \mathbb{R}^{12\times 1} \tag{8}$$

and

$$f(u) = -\begin{pmatrix} \mathbf{v} & 0 & 0 \\ 0 & \mathbf{v} & 0 \\ 0 & 0 & \mathbf{v} \\ \sigma(\mathbf{F})_1 & \sigma(\mathbf{F})_2 & \sigma(\mathbf{F})_3 \end{pmatrix} \in \mathbb{R}^{12\times 3}, \tag{9}$$

respectively. Derivatives are written according to custom as $D_{\mathbf{y}}g$, with $(D_{\mathbf{y}}g)_{ij} = \partial g_i/\partial y_j$. For short, $D_{(\mathbf{F},\mathbf{v})}g$ will denote $D_{(\mathbf{F}_1,\mathbf{F}_2,\mathbf{F}_3,\mathbf{v})}g$, for each function g. Given any function f of the state variables, we denote the jump across the interface as $[f] = f^+ - f^-$, and the mean value as $\langle f \rangle = \frac{1}{2}(f^+ + f^-)$.

Due to finite speed of propagation and the fact that we are interested in the local-in-time, local-in-space evolution near the interface, we assume for the rest of the paper that $\Omega = \mathbb{R}^3$, meaning no loss of generality.

1.1. Elastic phase boundaries

Suppose $(\mathbf{F}^+,\mathbf{v}^+)$ and $(\mathbf{F}^-,\mathbf{v}^-)$ are two constant states in $\mathbb{R}^{3\times 3}_+ \times \mathbb{R}^3$. Assume the energy density W is rank-one convex at $\mathbf{F} = \mathbf{F}^\pm$, that is, both the acoustic tensors $\mathbf{N}(\xi,\mathbf{F}^\pm)$ are positive definite for all $\xi \in \mathbb{R}^3$, $\xi \neq 0$ (Ciarlet, 1988), assuring that system (4) is hyperbolic in open neighborhoods of $\mathbf{F} = \mathbf{F}^\pm$ (see, e.g., Dafermos, 2005).

---

[1] Note that the (l,k)-component of the second-order tensor $\mathbf{B}_i^j$ is the $(ljki)$-entry of the fourth-order *elasticity* (or *stiffness*) tensor $\mathsf{A}_{ljki} = \partial^2 W/\partial \mathbf{F}_{lj} \partial \mathbf{F}_{ki}$ (Ciarlet, 1988).

Moving planar phase boundaries are weak solutions to system (4) of the form

$$(\mathbf{F}, \mathbf{v})(x, t) = \begin{cases} (\mathbf{F}^-, \mathbf{v}^-), & x \cdot \mathbf{n} - st < 0, \\ (\mathbf{F}^+, \mathbf{v}^+), & x \cdot \mathbf{n} - st > 0, \end{cases} \tag{10}$$

which travel at speed $s \in \mathbb{R}$ in the constant direction $\mathbf{n} \in \mathbb{R}^3, |\mathbf{n}| = 1, \mathbf{n} = (n_1, n_2, n_3)^\top$. These fronts satisfy canonical Rankine–Hugoniot jump conditions associated to Eqs. (4) and (5), having the form

$$-s[\mathbf{F}] - [\mathbf{v}] \otimes \mathbf{n} = 0,$$
$$-s[\mathbf{v}] - [\sigma(\mathbf{F})]\mathbf{n} = 0,$$
$$[\mathbf{F}] \times \mathbf{n} = 0, \tag{11}$$

and their speed s satisfies the *subsonicity condition*

$$0 \leqslant s^2 < \min\{\text{eigenvalues of } \mathbf{N}(\mathbf{n}, \mathbf{F}^\pm)\}. \tag{12}$$

Note that we have included the static case $s = 0$ into definition (12). The planar front travels in the direction of $\mathbf{n}$, which points out to the positive side by convention. If v_n denotes the velocity of propagation in the direction $\mathbf{n}$, then $v_n = s$. Under such assumptions, the planar front corresponds to an undercompressive shock (Freistühler, 1995), as the sum of the number of outgoing characteristics at both sides of the shock equals the dimension of the state space (in this case, $n = 12$, according to Eq. (8); see Freistühler and Plaza, 2007).

1.2. Kinetics

The speed s of such a subsonic planar phase boundary cannot be determined solely by Eqs. (4) and (11), and one needs one further jump condition. In the simplest case, a kinetic rule is given by an equation of the form

$$g((\mathbf{F}^-, \mathbf{v}^-), (\mathbf{F}^+, \mathbf{v}^+), s, \mathbf{n}) = 0, \tag{13}$$

interrelating the two states on either side (at some point) of the moving boundary with its space–time normal $(\mathbf{n}, s)$ (at that point). For non-planar moving phase boundaries, the same jump conditions apply pointwise. The precise circumstances under which the motion of phase boundaries in real materials can be captured by a kinetic rule of this simple kind, seem currently not clear from the literature. In the present paper we simply assume such circumstances and consider rules that, with some *regular* (at least once differentiable) real valued function

$$h = h((\mathbf{F}^-, \mathbf{v}^-), (\mathbf{F}^+, \mathbf{v}^+), s, \mathbf{n}),$$

are of form (13) with

$$g = \mathcal{F} + h, \tag{14}$$

$$\mathcal{F}(\mathbf{F}^+, \mathbf{F}^-, \mathbf{n}) := [W(\mathbf{F})] - \mathbf{n}^\top[\mathbf{F}]^\top \langle \sigma(\mathbf{F}) \rangle \mathbf{n}, \tag{15}$$

and compatible with some martensite twin (3) in the sense that

$$h((\underline{\mathbf{F}}^-, 0), (\underline{\mathbf{F}}^+, 0), 0, \nu) = 0. \tag{16}$$

Such kinetic rules (14) have been introduced by Abeyaratne and Knowles (1990, 1991) based on the principles of irreversible thermodynamics. The quantity $\mathcal{F}(\mathbf{F}^+, \mathbf{F}^-, \mathbf{n})$ is often called the *driving traction* (or *driving force*) across the boundary (Abeyaratne and Knowles, 1990). In its simplest form, a kinetic relation is given by $v_n = \phi(\mathcal{F})$, where ϕ is a (sometimes invertible) scalar valued function. In such cases it prescribes $\mathcal{F}$ as a function of the speed s, and determines the form of h above. In particular, the present study considers both the *Maxwell* (or *Hugoniot*) *rule*, corresponding to

$$h \equiv 0 \quad \text{identically}, \tag{17}$$

expressing conservation of energy across the interface, and *regular Abeyaratne– Knowles rules*, corresponding to h satisfying

$$h \text{ is a differentiable function of its parameters}, \tag{18a}$$

$$h((\cdot,\cdot),(\cdot,\cdot),0,\cdot) = 0 \quad \text{identically}, \tag{18b}$$

$$h > 0 \text{ for } s < 0, \quad h < 0 \text{ for } s > 0, \tag{18c}$$

$$(D_s h)_{|((\underline{\mathbf{F}}^-,0),(\underline{\mathbf{F}}^+,0),0,\boldsymbol{v})} < 0. \tag{18d}$$

The regularity assumption (18a) is one of the sufficient conditions for the analysis of Freistühler and Plaza (2007). In many kinetic models, condition (18b) is a common requirement at the static configuration (Abeyaratne and Knowles, 2006). Inequalities (18c) simply mean that the dissipation inequality

$$v_n \mathscr{F} \geqslant 0$$

holds, which is equivalent to imposing Clausius–Dulhem inequality along the interface (Abeyaratne and Knowles, 1990). Finally, condition (18d) is a sharper requirement on the static phase boundary inherited by the present stability study.

1.3. Stability of subsonic elastic phase boundaries

Assume Eq. (10) is a subsonic phase boundary satisfying Eq. (12), weak solution to Eq. (4), for which jump conditions (11) together with an already prescribed regular kinetic jump condition of form (13), hold. Suppose W is rank-one convex in open neighborhoods of $\mathbf{F} = \mathbf{F}^{\pm}$, and that the constant multiplicity condition of Métivier (2000) is satisfied (see Section 2.2 below for its precise statement).

The starting point of the stability analysis is the Fourier decomposition in normal modes of the constant coefficients linearized problem at the end states. For each $\mathbf{n} \in \mathbb{R}^3$, define the compact set of spatial-time (Fourier–Laplace) frequencies as

$$\mathscr{S} := \{(\lambda, \xi) \in \mathbb{C} \times \mathbb{R}^3 : \operatorname{Re}\lambda \geqslant 0, \xi \cdot \mathbf{n} = 0, |\lambda|^2 + |\xi|^2 = 1\},$$

with interior

$$\mathscr{S}^+ := \mathscr{S} \cap \{\operatorname{Re}\lambda > 0\}.$$

After linearizing system (4) at the end states and after shock localization (see, e.g., Majda, 1983a; Freistühler, 1998), one may substitute a normal mode ansatz of form

$$(\mathbf{F}^{\pm}, \mathbf{v}^{\pm})(x, t) = (\hat{\mathbf{F}}^{\pm}(x \cdot \mathbf{n} - st), \hat{\mathbf{v}}^{\pm}(x \cdot \mathbf{n} - st)) \, \mathrm{e}^{\mathrm{i}\xi \cdot x + \lambda t}, \tag{19}$$

for $x \cdot \mathbf{n} - st \gtrless 0$, and with $(\lambda, \xi) \in \mathscr{S}$, solution to both (4) and the constraint (5). The normal modes analysis of such solutions (Freistühler and Plaza, 2007) leads to the definition of the *reduced*[2] Lopatinski function

$$\Delta : \mathscr{S} \longrightarrow \mathbb{C}, \tag{20}$$

$$\Delta(\lambda, \xi) = \det \begin{pmatrix} \hat{\mathbf{R}}^{\mathrm{s}}(\mathbf{F}^-) & \hat{Q} & \hat{\mathbf{R}}^{\mathrm{u}}(\mathbf{F}^+) \\ \hat{p}^- & \hat{q} & \hat{p}^+ \end{pmatrix}, \tag{21}$$

where

$$\hat{Q}(\lambda, \xi) = \begin{pmatrix} [\mathbf{F}]\mathbf{n} \\ -\lambda s[\mathbf{F}]\mathbf{n} - \mathrm{i}[\sigma(\mathbf{F})]\xi \end{pmatrix} \in \mathbb{C}^{6 \times 1},$$

$$\hat{q}(\lambda, \xi) = -\lambda(D_s g) + \mathrm{i}(\xi \cdot D_{\mathbf{n}}g) \in \mathbb{C}^{1 \times 1},$$

$$\hat{p}^-(\lambda, \xi) = -(D_{(\mathbf{F}^-,\mathbf{v}^-)}g)\mathscr{K}_{s,\mathbf{n}}(\mathbf{F}^-)\hat{\mathbf{R}}^{\mathrm{s}}(\mathbf{F}^-) \in \mathbb{C}^{1 \times 3},$$

$$\hat{p}^+(\lambda, \xi) = (D_{(\mathbf{F}^+,\mathbf{v}^+)}g)\mathscr{K}_{s,\mathbf{n}}(\mathbf{F}^+)\hat{\mathbf{R}}^{\mathrm{s}}(\mathbf{F}^+) \in \mathbb{C}^{1 \times 3}.$$

---

[2] We call it *reduced* in the sense that its definition is restricted to the invariant subspace of normal modes (19) satisfying the constraint (5).

Here $\hat{\mathbf{R}}^{\mathrm{s,u}}(\mathbf{F}) \in \mathbb{C}^{6\times 1}$ represent the right stable and unstable invariant spaces of a matrix field $\mathbb{M}_{s,\mathbf{n}}(\mathbf{F}) : \mathscr{S} \to \mathbb{C}^{6\times 6}$ for each $\mathbf{F}$ near $\mathbf{F}^{\pm}$, and $\mathscr{K}_{s,\mathbf{n}}(\mathbf{F}) : \mathscr{S} \to \mathbb{C}^{12\times 6}$ denote continuous mappings. $\mathbb{M}$ and $\mathscr{K}$ are given by explicit formulae in terms of the first and second derivatives of the energy function W (for their precise form in the case of a static interface, see Section 3; for the general case of a dynamic phase boundary, the reader is referred to Freistühler and Plaza, 2007). In Eq. (21), $\hat{Q}$ is the "jump vector" associated to Rankine–Hugoniot conditions (Majda, 1983a), and $\hat{q}$ denotes its kinetic counterpart (Freistühler, 1998). All elements in Eq. (21) are evaluated at the end states $(\mathbf{F}^{\pm}, \mathbf{v}^{\pm}, s, \mathbf{n})$ and depend continuously on its parameters for all subsonic s including $s = 0$. Furthermore, as a function of (λ, ξ), $\varDelta$ is analytic in $\mathscr{S}^{+}$ and continuous in the whole set $\mathscr{S}$.

In spite of its somewhat convoluted definition, the significance of $\varDelta$ is precisely that it measures the solvability of the linearized system by wave solutions that violate the well-posedness L^2-estimate of Kreiss (for its precise form, see Majda, 1983a; Métivier, 1990). Whenever a zero of $\varDelta$ occurs, the intersection of initial conditions at $z := x \cdot \mathbf{n} - st = 0$ that accept spatially decaying solutions as $z \to \pm\infty$ is non-trivial, and a solution with time growth rate $\exp(t\,\mathrm{Re}\,\lambda)$ exists. Therefore, one may verify that a necessary condition for well-posedness of the linearized problem is that $\varDelta$ does not vanish in the interior set $\mathscr{S}^{+}$. In this case we say that $\varDelta$ satisfies the Lopatinski condition, and that the front is *weakly stable*. Zeroes of $\varDelta$ along the imaginary axis $(\lambda, \xi) \in \mathscr{S} \cap \{\mathrm{Re}\,\lambda = 0\}$ for weakly stable interfaces refer to the existence of surface waves localized near $z = 0$. A stronger condition, called the *uniform* Lopatinski condition, namely, that $\varDelta$ has no zeroes in the whole set $\mathscr{S}$ (including the imaginary axis $\{\mathrm{Re}\,\lambda = 0\}$), ensures the well-posedness of the nonlinear system. In this case, we say the front is *uniformly* (or *strongly*) *stable*. Finally, when $\varDelta$ vanishes for some point in $\mathscr{S}^{+}$, we say the front is *strongly unstable*. In this last case the instability is of Hadamard type and it is so violent that we never observe the discontinuity evolve in time.

1.4. Main results

The goal of this paper is to show that at least one widely considered example of a martensite twin is weakly stable under the Maxwell rule (17), and uniformly stable under regular Abeyaratne–Knowles rules (18). Following Ball and James (1987), the example we have chosen twins two *monoclinic* deformations

$$\underline{\mathbf{F}}^{+} = \begin{pmatrix} 1 & 0 & 0 \\ \varepsilon & 1 & 0 \\ 0 & 0 & 1 \end{pmatrix} \quad \text{and} \quad \underline{\mathbf{F}}^{-} = \begin{pmatrix} 1 & 0 & 0 \\ -\varepsilon & 1 & 0 \\ 0 & 0 & 1 \end{pmatrix}, \tag{22}$$

for a material parameter $\varepsilon > 0$, which are clearly rank-one connected,

$$\underline{\mathbf{F}}^{+} - \underline{\mathbf{F}}^{-} = 2\varepsilon\hat{e}_2 \otimes \hat{e}_1,$$

and satisfy $\det \underline{\mathbf{F}}^{+} = \det \underline{\mathbf{F}}^{-} = 1$. The rotationally invariant energy wells are defined by

$$\mathscr{U}^{+} = \mathrm{SO}(3)\underline{\mathbf{F}}^{+}, \quad \mathscr{U}^{-} = \mathrm{SO}(3)\underline{\mathbf{F}}^{-},$$

where

$$\mathrm{SO}(3) = \{\mathbf{Q} \in \mathbb{R}^{3\times 3} : \mathbf{Q}^{\top}\mathbf{Q} = \mathbf{I},\ \det \mathbf{Q} = 1\}$$

is the group of proper rotations. As the stored-energy function, we concretely take

$$W(\mathbf{F}) = \frac{1}{32} \left| \mathbf{C} - \begin{pmatrix} 1+\varepsilon^2 & \varepsilon & 0 \\ \varepsilon & 1 & 0 \\ 0 & 0 & 1 \end{pmatrix} \right|^2 \left| \mathbf{C} - \begin{pmatrix} 1+\varepsilon^2 & -\varepsilon & 0 \\ -\varepsilon & 1 & 0 \\ 0 & 0 & 1 \end{pmatrix} \right|^2, \tag{23}$$

where $\mathbf{C}(\mathbf{F}) = \mathbf{F}^{\top}\mathbf{F}$ is the right Cauchy–Green strain, and $|\cdot|$ denotes the Frobenius norm on $\mathbb{R}^{3\times 3}$,

$$|\mathbf{M}|^2 = \mathrm{Tr}\,(\mathbf{M}^{\top}\mathbf{M}).$$

Function (23) is frame-indifferent, as $W(\mathbf{Q}\mathbf{F}) = W(\mathbf{F})$ for all $\mathbf{Q} \in \mathrm{SO}(3)$, and attains its minimum only on the set $\mathscr{U} = \mathscr{U}^{-} \cup \mathscr{U}^{+}$, that is, $W(\mathbf{F}) = 0$ if and only if $\mathbf{F} \in \mathscr{U}$. This energy density, a choice following Kružík and Luskin (2003), is an example of the simplest multiple well structure where the number of different variants is 2, namely, a double-well energy modelling orthorhombic-to-monoclinic transformations (Ball and James, 1992).

For this particular material, we numerically evaluate the Lopatinski function Δ associated to Eqs. (22) and (23), and find that, (*i*) *with Maxwell kinetics, Δ has zeroes on the boundary of $\mathcal{S}$ and no zeroes in the interior of $\mathcal{S}$ (weak stability), while, (ii) with various choices of regular Abeyaratne– Knowles kinetics, Δ has no zeroes on all of $\mathcal{S}$ (uniform stability).*

2. Energy density function and kinetic rules

This section gathers properties of the energy density function (23) and the kinetic rules (17) and (18), which are needed for the computation of the stability function.

2.1. Derivatives of the stress

First, we compute the matrices $\mathbf{B}_i^j$ containing the second derivatives of the energy. Denoting $\Phi_\pm(\mathbf{F}) := |\mathbf{C} - \mathbf{C}^\pm|^2$, then clearly $W(\mathbf{F}) = \frac{1}{32}\Phi_+(\mathbf{F})\Phi_-(\mathbf{F})$, with $\Phi_\pm(\underline{\mathbf{F}}^\pm) = 0$ and $\Phi_\pm(\underline{\mathbf{F}}^\mp) = 8\varepsilon^2 > 0$. By direct computation,

$$(D_{\mathbf{F}_1}\Phi_\pm)(\mathbf{F}) = 4((|\mathbf{F}_1|^2 - (1+\varepsilon^2))\mathbf{F}_1 + (\mathbf{F}_2^\top\mathbf{F}_1 \mp \varepsilon)\mathbf{F}_2 + (\mathbf{F}_1^\top\mathbf{F}_3)\mathbf{F}_3),$$
$$(D_{\mathbf{F}_2}\Phi_\pm)(\mathbf{F}) = 4((|\mathbf{F}_2|^2 - 1)\mathbf{F}_2 + (\mathbf{F}_2^\top\mathbf{F}_1 \mp \varepsilon)\mathbf{F}_1 + (\mathbf{F}_2^\top\mathbf{F}_3)\mathbf{F}_3),$$
$$(D_{\mathbf{F}_3}\Phi_\pm)(\mathbf{F}) = 4((|\mathbf{F}_3|^2 - 1)\mathbf{F}_2 + (\mathbf{F}_3^\top\mathbf{F}_1 \mp \varepsilon)\mathbf{F}_1 + (\mathbf{F}_2^\top\mathbf{F}_3)\mathbf{F}_2). \tag{24}$$

Since the stress σ vanishes at the wells, it is easy to see that for all i,j,

$$\mathbf{B}_i^{j\pm} = \tfrac{1}{32}\Phi_\mp(\underline{\mathbf{F}}^\pm)(D^2_{\mathbf{F}_j\mathbf{F}_i}\Phi_\pm)(\underline{\mathbf{F}}^\pm) = \tfrac{1}{4}\varepsilon^2(D^2_{\mathbf{F}_j\mathbf{F}_i}\Phi_\pm)(\underline{\mathbf{F}}^\pm).$$

From Eq. (24) we obtain

$$(D^2_{\mathbf{F}_1\mathbf{F}_1}\Phi_\pm)(\mathbf{F}) = 4(2\mathbf{F}_1 \otimes \mathbf{F}_1 + (|\mathbf{F}_1|^2 - (1+\varepsilon^2))\mathbf{I} + \mathbf{F}_2 \otimes \mathbf{F}_2 + \mathbf{F}_3 \otimes \mathbf{F}_3),$$
$$(D^2_{\mathbf{F}_2\mathbf{F}_2}\Phi_\pm)(\mathbf{F}) = 4(2\mathbf{F}_2 \otimes \mathbf{F}_2 + (|\mathbf{F}_2|^2 - 1)\mathbf{I} + \mathbf{F}_1 \otimes \mathbf{F}_1 + \mathbf{F}_3 \otimes \mathbf{F}_3),$$
$$(D^2_{\mathbf{F}_3\mathbf{F}_3}\Phi_\pm)(\mathbf{F}) = 4(2\mathbf{F}_3 \otimes \mathbf{F}_3 + (|\mathbf{F}_3|^2 - 1)\mathbf{I} + \mathbf{F}_1 \otimes \mathbf{F}_1 + \mathbf{F}_2 \otimes \mathbf{F}_2),$$
$$(D^2_{\mathbf{F}_1\mathbf{F}_2}\Phi_\pm)(\mathbf{F}) = (D^2_{\mathbf{F}_2\mathbf{F}_1}\Phi_\pm)^\top = 4(\mathbf{F}_1 \otimes \mathbf{F}_2 + (\mathbf{F}_2^\top\mathbf{F}_1 \mp \varepsilon)\mathbf{I}),$$
$$(D^2_{\mathbf{F}_1\mathbf{F}_3}\Phi_\pm)(\mathbf{F}) = (D^2_{\mathbf{F}_3\mathbf{F}_1}\Phi_\pm)^\top = 4(\mathbf{F}_1 \otimes \mathbf{F}_3 + (\mathbf{F}_1^\top\mathbf{F}_3)\mathbf{I}),$$
$$(D^2_{\mathbf{F}_2\mathbf{F}_3}\Phi_\pm)(\mathbf{F}) = (D^2_{\mathbf{F}_2\mathbf{F}_1}\Phi_\pm)^\top = 4(\mathbf{F}_2 \otimes \mathbf{F}_3 + (\mathbf{F}_2^\top\mathbf{F}_3)\mathbf{I}), \tag{25}$$

and evaluating at the wells we readily get,

$$\mathbf{B}_1^{1\pm} = \varepsilon^2\begin{pmatrix} 2 & \pm2\varepsilon & 0 \\ \pm2\varepsilon & 1+2\varepsilon^2 & 0 \\ 0 & 0 & 1 \end{pmatrix}, \quad \mathbf{B}_2^{1\pm} = (\mathbf{B}_1^{2\pm})^\top = \varepsilon^2\begin{pmatrix} 0 & 1 & 0 \\ 0 & \pm\varepsilon & 0 \\ 0 & 0 & 0 \end{pmatrix},$$

$$\mathbf{B}_2^{2\pm} = \varepsilon^2\begin{pmatrix} 1 & \pm\varepsilon & 0 \\ \pm\varepsilon & 2+\varepsilon^2 & 0 \\ 0 & 0 & 1 \end{pmatrix}, \quad \mathbf{B}_3^{1\pm} = (\mathbf{B}_1^{3\pm})^\top = \varepsilon^2\begin{pmatrix} 0 & 0 & 1 \\ 0 & 0 & \pm\varepsilon \\ 0 & 0 & 0 \end{pmatrix},$$

$$\mathbf{B}_3^{3\pm} = \varepsilon^2\begin{pmatrix} 1 & \pm\varepsilon & 0 \\ \pm\varepsilon & 1+\varepsilon^2 & 0 \\ 0 & 0 & 2 \end{pmatrix}, \quad \mathbf{B}_3^{2\pm} = (\mathbf{B}_2^{3\pm})^\top = \varepsilon^2\begin{pmatrix} 0 & 0 & 0 \\ 0 & 0 & 1 \\ 0 & 0 & 0 \end{pmatrix}. \tag{26}$$

From Eq. (26) one finds that

$$(\mathbf{B}_1^{1\pm})^{-1} = \varepsilon^{-2} \begin{pmatrix} \frac{1}{2}(1 + 2\varepsilon^2) & \mp\varepsilon & 0 \\ \mp\varepsilon & 1 & 0 \\ 0 & 0 & 1 \end{pmatrix}. \tag{27}$$

Note that the eigenvalues of $\mathbf{B}_1^{1\pm}$ are

$$k_1 = \frac{1}{2}\varepsilon^2\left(3 + 2\varepsilon^2 - \sqrt{(3 + 2\varepsilon^2)^2 - 8}\right),$$
$$k_2 = \varepsilon^2,$$
$$k_3 = \frac{1}{2}\varepsilon^2\left(3 + 2\varepsilon^2 + \sqrt{(3 + 2\varepsilon^2)^2 - 8}\right), \tag{28}$$

with $0 < k_1 < k_2 < k_3$ and constant multiplicity 1. Therefore, the six characteristic speeds associated to the front are $\alpha_j = \pm\sqrt{k_j}$, $j = 1, 2, 3$. The analysis of Freistühler and Plaza (2007) applies to all subsonic propagating fronts with speed satisfying $0 \leqslant s^2 < k_j$ for all j.

2.2. Rank-one convexity and constant multiplicity assumption

In this subsection, we verify two hypotheses made by Freistühler and Plaza (2007), so as to guarantee that the results of our computations really allow for the said conclusions. To ensure hyperbolicity at the end states, the first hypothesis is the rank-one convexity of W at the wells, or equivalently, that *Legendre–Hadamard condition*,

$$\zeta^\top \mathbf{N}(\xi, \underline{\mathbf{F}}^\pm)\zeta > 0 \quad \text{for all } \zeta, \xi \in \mathbb{R}^3\backslash\{0\}, \tag{29}$$

holds (Ciarlet, 1988). In order to verify Eq. (29) we express W in terms of the right Cauchy–Green strain as

$$W =: \hat{W}(C_{11}, C_{22}, C_{33}, C_{12}, C_{13}, C_{23}),$$

with Hessian

$$(D_\mathbf{C}^2 \hat{W})_{|\mathbf{C}=\mathbf{C}^\pm} = \varepsilon^2 \begin{pmatrix} \frac{1}{2}\mathbf{I} & 0 \\ 0 & \mathbf{I} \end{pmatrix} > 0,$$

for all $\varepsilon > 0$ and evaluated, of course, at the minima $\mathbf{C} = \mathbf{C}^\pm$. Therefore, it is easy to see that the quadratic form in Eq. (29) can be written as

$$b^\pm(\xi, \zeta) := \zeta^\top \mathbf{N}(\xi, \underline{\mathbf{F}}^\pm)\zeta = \xi^\top \mathbf{H}(\underline{\mathbf{F}}^\pm, \zeta)^\top (D_\mathbf{C}^2 \hat{W})_{|\mathbf{C}=\mathbf{C}^\pm} \mathbf{H}(\underline{\mathbf{F}}^\pm, \zeta)\xi,$$

where the 6×3 matrix $\mathbf{H}(\underline{\mathbf{F}}^\pm, \zeta)$ is defined by

$$\mathbf{H}(\underline{\mathbf{F}}^\pm, \zeta) = \begin{pmatrix} 2(\underline{\mathbf{F}}_1^\pm)^\top \zeta & 0 & 0 \\ 0 & 2(\underline{\mathbf{F}}_2^\pm)^\top \zeta & 0 \\ 0 & 0 & 2(\underline{\mathbf{F}}_3^\pm)^\top \zeta \\ (\underline{\mathbf{F}}_2^\pm)^\top \zeta & (\underline{\mathbf{F}}_1^\pm)^\top \zeta & 0 \\ (\underline{\mathbf{F}}_3^\pm)^\top \zeta & 0 & (\underline{\mathbf{F}}_1^\pm)^\top \zeta \\ 0 & (\underline{\mathbf{F}}_3^\pm)^\top \zeta & (\underline{\mathbf{F}}_2^\pm)^\top \zeta \end{pmatrix}.$$

Since for each $\zeta \neq 0$, $\mathbf{H}(\underline{\mathbf{F}}^\pm, \zeta)$ has full rank (as $\det \underline{\mathbf{F}}^\pm > 0$) and in view of $(D_\mathbf{C}^2 \hat{W})_{|\mathbf{C}=\mathbf{C}^\pm} > 0$, then clearly $b^\pm(\xi, \zeta) > 0$ for all $\zeta, \xi \in \mathbb{R}^3\backslash\{0\}$, that is, W is rank-one convex at $\mathbf{F} = \underline{\mathbf{F}}^\pm$ and the system is hyperbolic in open neighborhoods of the two wells.

Another (though actually not essential) requirement for the analysis is the constant multiplicity condition of Métivier (2000), namely, that the eigenvalues of $\mathbf{N}(\xi, \mathbf{F})$ are all semi-simple (the algebraic and geometric multiplicities coincide) with constant multiplicities for all $\mathbf{F}$ near $\underline{\mathbf{F}}^+$ or $\underline{\mathbf{F}}^-$, and for all $\xi \neq 0$. By continuity of the eigenvalues, it suffices to check this condition at the wells, as the property is preserved in open

neighborhoods of $\mathbf{F} = \underline{\mathbf{F}}^{\pm}$. Notice that $\mathbf{N}(\rho\xi, \underline{\mathbf{F}}^{\pm}) = \rho^2\mathbf{N}(\xi, \underline{\mathbf{F}}^{\pm})$ for all $\rho > 0$. Hence, after normalization, it suffices to consider $|\xi| = 1$ which we parametrize in spherical coordinates by $\xi_1 = \sin\psi\cos\theta$, $\xi_2 = \sin\psi\sin\theta$, and $\xi_3 = \cos\psi$, with $\theta \in [0, 2\pi]$, $\psi \in [0, \pi]$. One can easily check Métivier's condition numerically and find that it is satisfied by the energy (23) at the wells (22) within an open set of the material parameter ε containing the segment [0.5, 1]. For instance, Fig. 1 shows the computed eigenvalues κ_j of $\mathbf{N}(\xi, \underline{\mathbf{F}}^{\pm})$, for $\varepsilon = 0.5$, in a mesh of angles (ψ, θ), smoothly interpolated as surfaces. It turns out that the eigenvalues are all simple for each value of ξ.

2.3. Derivatives of kinetic rules

In this section we gather the derivatives of h and $\mathscr{F}$ from Eqs. (16)–(18), with respect to their parameters $(\underline{\mathbf{F}}^+, \mathbf{v}^+), (\underline{\mathbf{F}}^-, \mathbf{v}^-)$, $\mathbf{n}$, and s. Noticing that for each i, j, we have

$$\partial_{\mathbf{F}_{ij}^{\pm}}(\mathbf{n}^{\top}[\mathbf{F}]^{\top}\langle\sigma(\mathbf{F})\rangle\mathbf{n}) = \pm n_j\sum_k n_k\langle\sigma(\mathbf{F})_{ik}\rangle + \frac{1}{2}\mathbf{n}^{\top}[\mathbf{F}]^{\top}\sum_l n_l\,\partial_{\mathbf{F}_{ij}^{\pm}}(\sigma(\mathbf{F}^{\pm})_l)$$

$$= \pm n_j\sum_k n_k\langle\sigma(\mathbf{F})_{ik}\rangle + \frac{1}{2}\sum_{l,k} n_l([\mathbf{F}]\mathbf{n})_k(\mathbf{B}_j^{l\pm})_{ki},$$

one gets,

$$D_{(\mathbf{F}^{\pm}, \mathbf{v}^{\pm})}\mathscr{F} = \left(\pm\sigma(\mathbf{F}^{\pm})_1^{\top} \mp n_1\mathbf{n}^{\top}\langle\sigma(\mathbf{F})\rangle^{\top} - \frac{1}{2}\mathbf{n}^{\top}[\mathbf{F}]^{\top}\sum_{j=1}^{3} n_j\mathbf{B}_1^{j\pm}, \right.$$

$$\pm\sigma(\mathbf{F}^{\pm})_2^{\top} \mp n_2\mathbf{n}^{\top}\langle\sigma(\mathbf{F})\rangle^{\top} - \frac{1}{2}\mathbf{n}^{\top}[\mathbf{F}]^{\top}\sum_{j=1}^{3} n_j\mathbf{B}_2^{j\pm},$$

$$\left.\pm\sigma(\mathbf{F}^{\pm})_3^{\top} \mp n_3\mathbf{n}^{\top}\langle\sigma(\mathbf{F})\rangle^{\top} - \frac{1}{2}\mathbf{n}^{\top}[\mathbf{F}]^{\top}\sum_{j=1}^{3} n_j\mathbf{B}_3^{j\pm}, \; 0\right) \in \mathbb{R}^{1\times 12} \tag{30}$$

(where each element is a 1×3 block), and

$$D_{\mathbf{n}}\mathscr{F} = \mathbf{n}^{\top}([\mathbf{F}]^{\top}\langle\sigma(\mathbf{F})\rangle + \langle\sigma(\mathbf{F})\rangle^{\top}[\mathbf{F}]) \in \mathbb{R}^{1\times 3}, \tag{31}$$
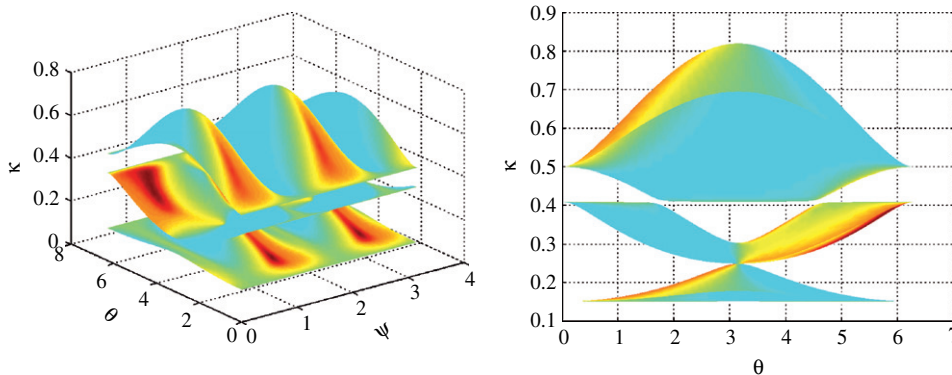
$$D_s\mathscr{F} \equiv 0. \tag{32}$$

Fig. 1. Plot of the eigenvalues of $\mathbf{N}(\xi, \underline{\mathbf{F}}^{\pm})$, $\xi = (\sin\psi\cos\theta, \sin\psi\sin\theta, \cos\psi)$ on a mesh $(\psi, \theta) \in [0, \pi] \times [0, 2\pi]$. We set the material parameter as $\varepsilon = 0.5$. The three surfaces correspond to the continuous values of the three real eigenvalues κ_j, $j = 1, 2, 3$. The azimuthal view on the right shows that the eigenvalues are simple and never coalesce.

Furthermore, we obviously have

$$\begin{aligned} D_{(\mathbf{F}^\pm, \mathbf{v}^\pm)} h &= 0 \\ D_{\mathbf{n}} h &= 0 \end{aligned} \quad \text{at } ((\underline{\mathbf{F}}^+, 0), (\underline{\mathbf{F}}^-, 0), 0, \hat{e}_1), \tag{33}$$

both for Maxwell and Abeyaratne–Knowles rules.

3. The reduced Lopatinski function for a martensite twin

In view of our choice of the wells (22), let us assume that the normal to the static front (3) points out in the direction of the x_1-axis, that is, that $\mathbf{v} = \hat{e}_1$. The transversal directions are thus given by $\xi = (0, \xi_2, \xi_3)^\top$ with $\xi_1 = 0$; we define then $\check{\xi} := (\xi_2, \xi_3) \in \mathbb{R}^2$ so that the set $\mathscr{S}$ of space–time frequencies can be expressed as

$$\mathscr{S} = \{(\lambda, \check{\xi}) \in \mathbb{C} \times \mathbb{R}^2 : |\lambda|^2 + |\check{\xi}|^2 = 1, \operatorname{Re} \lambda \geqslant 0\}, \tag{34}$$

with interior,

$$\mathscr{S}^+ = \mathscr{S} \cap \{\operatorname{Re} \lambda > 0\}.$$

Consider the two continuous matrix fields $\mathbb{M}_\pm : \mathscr{S} \to \mathbb{C}^{6\times 6}$ defined by

$$\mathbb{M}_\pm(\lambda, \check{\xi}) := \begin{pmatrix} \mathbf{M}_{11}^\pm & \mathbf{M}_{12}^\pm \\ \mathbf{M}_{21}^\pm & \mathbf{M}_{22}^\pm \end{pmatrix}, \quad \mathbf{M}_{ij}^\pm : \mathscr{S} \to \mathbb{C}^{3\times 3}, \tag{35}$$

with

$$\begin{aligned}
\mathbf{M}_{11}^\pm &= i(\mathbf{B}_1^{1\pm})^{-1}(\xi_2 \mathbf{B}_2^{1\pm} + \xi_3 \mathbf{B}_3^{1\pm}), \\
\mathbf{M}_{12}^\pm &= -(\mathbf{B}_1^{1\pm})^{-1}, \\
\mathbf{M}_{21}^\pm &= (\xi_2 \mathbf{B}_1^{2\pm} + \xi_3 \mathbf{B}_1^{3\pm})(\mathbf{B}_1^{1\pm})^{-1}(\xi_2 \mathbf{B}_2^{1\pm} + \xi_3 \mathbf{B}_3^{1\pm}) - \lambda^2 \mathbf{I} - (\xi_2^2 \mathbf{B}_2^{2\pm} + \xi_3^2 \mathbf{B}_3^{3\pm} + \xi_2 \xi_3 (\mathbf{B}_3^{2\pm} + \mathbf{B}_2^{3\pm})), \\
\mathbf{M}_{22}^\pm &= i(\xi_2 \mathbf{B}_1^{2\pm} + \xi_3 \mathbf{B}_1^{3\pm})(\mathbf{B}_1^{1\pm})^{-1}.
\end{aligned} \tag{36}$$

The main observation of Freistühler and Plaza (2007) is that the curl-free constraint (5) reduces the normal modes analysis for the stability of such elastic fronts to a subspace of amplitudes, whose dynamics in the frequency (or Fourier–Laplace) space is captured by the matrix fields $\mathbb{M}_\pm$. In view of their analysis, the stability function (21) for such a static planar interface takes the form

$$\Delta(\lambda, \check{\xi}) = \det \begin{pmatrix} \hat{\mathbf{R}}_-^{\mathrm{s}} & \hat{Q} & \hat{\mathbf{R}}_+^{\mathrm{u}} \\ \hat{p}^- & \hat{q} & \hat{p}^+ \end{pmatrix}, \tag{37}$$

where

$$\hat{Q} = \begin{pmatrix} [\mathbf{F}_1] \\ i[\sigma(\mathbf{F})](0, \check{\xi})^\top \end{pmatrix} \in \mathbb{C}^{6\times 1}, \tag{38}$$

$$\hat{q} = -\lambda(D_s g) + i((0, \check{\xi})^\top(D_{\mathbf{n}} g)) \in \mathbb{C}^{1\times 1}, \tag{39}$$

$$\begin{aligned}
\hat{p}^+ &= (D_{(\mathbf{F}^+, \mathbf{v}^+)} g) \mathscr{K}_+(\lambda, \check{\xi}) \hat{\mathbf{R}}_+^{\mathrm{u}} \in \mathbb{C}^{1\times 3}, \\
\hat{p}^- &= -(D_{(\mathbf{F}^-, \mathbf{v}^-)} g) \mathscr{K}_-(\lambda, \check{\xi}) \hat{\mathbf{R}}_-^{\mathrm{s}} \in \mathbb{C}^{1\times 3},
\end{aligned} \tag{40}$$

$$\mathscr{K}_\pm(\lambda, \check{\xi}) = \begin{pmatrix} i(\mathbf{B}_1^{1\pm})^{-1}(\xi_2 \mathbf{B}_2^{1\pm} + \xi_3 \mathbf{B}_3^{1\pm}) & -(\mathbf{B}_1^{1\pm})^{-1} \\ -i\xi_2 \mathbf{I} & 0 \\ -i\xi_3 \mathbf{I} & 0 \\ -\lambda \mathbf{I} & 0 \end{pmatrix} \in \mathbb{C}^{12\times 6}, \tag{41}$$

and $\hat{\mathbf{R}}_+^{\mathrm{u}} = \hat{\mathbf{R}}_+^{\mathrm{u}}(\lambda, \check{\xi}) \in \mathbb{C}^{6\times 3}$ (resp. $\hat{\mathbf{R}}_-^{\mathrm{s}}$) denotes the unstable (resp. stable) space of the matrix field $\mathbb{M}_+$ (resp. $\mathbb{M}_-$). All these elements are evaluated, of course, at the wells, for which W attains its minima, and at $s = 0$. In addition, Δ is analytic in $(\lambda, \check{\xi}) \in \mathscr{S}^+$ and continuous in $(\lambda, \check{\xi}) \in \mathscr{S}$.

3.1. Stable and unstable modes

For convenience, let us denote $\mathbf{N}_\pm(\mu, \tilde{\xi}) := \mathbf{N}(\mu, \xi_2, \xi_3, \underline{\mathbf{F}}^\pm)$, where ξ_1 has been replaced by a complex parameter $\mu \in \mathbb{C}$ in expression (7). It has been shown that the eigenvalues $\beta = -i\mu$ of $\mathbb{M}_\pm$ satisfy the following characteristic equation:

$$\pi_\pm(\mu) := \det(\mathbf{N}_\pm(\mu, \tilde{\xi}) + \lambda^2 \mathbf{I}) = 0, \tag{42}$$

for all $(\lambda, \tilde{\xi}) \in \mathscr{S}$. Moreover, restricting to $\mathscr{S}^+$, and due to hyperbolicity at the end states, the eigenvalues split into *stable* (with $\operatorname{Im}\mu < 0$) and *unstable* (with $\operatorname{Im}\mu > 0$) modes. This hyperbolic dichotomy in the dynamical systems sense was originally pointed out by Hersh (1963). Under the current assumptions, there are exactly three unstable and three stable eigenmodes (counting multiplicities) for each $(\lambda, \tilde{\xi}) \in \mathscr{S}^+$, implying that the stable and unstable spaces of both $\mathbb{M}_\pm$ have constant dimension in all $\mathscr{S}^+$. These invariant right spaces are represented by mappings (or bundles) $\hat{\mathbf{R}}_\pm^{\mathrm{s,u}} : \mathscr{S} \to \mathbb{C}^{6 \times 3}$ arranged in suitable column bases which can be chosen analytic on $\mathscr{S}^+$ with continuous extensions to all of $\mathscr{S}$. For details, see Freistühler and Plaza (2007) and the references therein.

From Lemma 6 in the same reference, we reckon that the eigenvector of $\mathbb{M}_\pm$ associated to an eigenvalue $\beta = -i\mu$ has the form

$$\mathbf{r} = \begin{pmatrix} \mathbf{w} \\ i(\mu \mathbf{B}_1^{1\pm} + \xi_2 \mathbf{B}_2^{1\pm} + \xi_3 \mathbf{B}_3^{1\pm})\mathbf{w} \end{pmatrix}, \tag{43}$$

where

$$\mathbf{w} \in \ker(\mathbf{N}_\pm(\mu, \tilde{\xi}) + \lambda^2 \mathbf{I}). \tag{44}$$

3.2. Kinetic rule and jump conditions blocks

In this section we compute the elements in Δ associated to the classical jump conditions and the kinetic rule. First, since $\sigma = 0$ at the wells, we have

$$\hat{Q} = \begin{pmatrix} \underline{\mathbf{F}}_1^+ - \underline{\mathbf{F}}_1^- \\ 0 \end{pmatrix} = 2\varepsilon \begin{pmatrix} \hat{e}_2 \\ 0 \end{pmatrix} \in \mathbb{R}^{6 \times 1}.$$

Recalling expressions (30) and (31), specializing them to the case where $\mathbf{n} = \hat{e}_1$, evaluating at the wells, and using Eq. (26), we arrive at

$$\begin{aligned}
(D_s g)_{|s=0} &= D_s(\mathscr{F} + h)_{s=0} = (D_s h)_{|s=0}, \\
(D_\mathbf{n} g)_{|s=0} &= D_\mathbf{n}(\mathscr{F} + h)_{s=0} = 0, \\
(D_{(\mathbf{F}^\pm, \mathbf{v}^\pm)} g)_{|s=0} &= D_{(\mathbf{F}^\pm, \mathbf{v}^\pm)}(\mathscr{F} + h)_{|s=0} \\
&= (-\tfrac{1}{2}[\underline{\mathbf{F}}_1]^\top \mathbf{B}_1^{1\pm}, -\tfrac{1}{2}[\underline{\mathbf{F}}_1]^\top \mathbf{B}_2^{1\pm}, -\tfrac{1}{2}[\underline{\mathbf{F}}_1]^\top \mathbf{B}_3^{1\pm}, 0) \\
&= -\varepsilon^3((\pm 2\varepsilon, 1 + 2\varepsilon^2, 0), \pm \varepsilon \hat{e}_2^\top, \pm \varepsilon \hat{e}_3^\top, 0) \in \mathbb{R}^{1 \times 12}.
\end{aligned}$$

Using Eqs. (26) and (27), we also compute

$$\mathscr{K}_\pm(\lambda, \tilde{\xi}) = \begin{pmatrix} \dfrac{i}{2}\begin{pmatrix} 0 & \xi_2 & \xi_3 \\ 0 & 0 & 0 \\ 0 & 0 & 0 \end{pmatrix} & \varepsilon^{-2}\begin{pmatrix} -\tfrac{1}{2}(1 + 2\varepsilon^2) & \pm\varepsilon & 0 \\ \pm\varepsilon & -1 & 0 \\ 0 & 0 & -1 \end{pmatrix} \\ -i\xi_2 \mathbf{I} & 0 \\ -i\xi_3 \mathbf{I} & 0 \\ -\lambda \mathbf{I} & 0 \end{pmatrix}.$$

Hence,

$$
\begin{aligned}
(D_{(\mathbf{F}^+, v^+)}g)_{|s=0}\mathscr{K}_+(\lambda, \tilde{\xi}) &= -\varepsilon^3((2\varepsilon, 1 + 2\varepsilon^2, 0), \varepsilon\hat{e}_2^\top, \varepsilon\hat{e}_3^\top, 0)\mathscr{K}_+(\lambda, \tilde{\xi}) \\
&= \varepsilon(0, \hat{e}_2^\top) \in \mathbb{R}^{1\times 6}, \\
(D_{(\mathbf{F}^-, v^-)}g)_{|s=0}\mathscr{K}_-(\lambda, \tilde{\xi}) &= -\varepsilon^3((-2\varepsilon, 1 + 2\varepsilon^2, 0), -\varepsilon\hat{e}_2^\top, -\varepsilon\hat{e}_3^\top, 0)\mathscr{K}_-(\lambda, \tilde{\xi}) \\
&= \varepsilon(0, \hat{e}_2^\top) \in \mathbb{R}^{1\times 6}.
\end{aligned}
$$

3.3. Using the symmetry of the twin

Thanks to the symmetries associated to the martensitic wells, we can simplify the expression for Δ. For instance, let

$$
\Pi = \begin{pmatrix} 1 & 0 & 0 \\ 0 & -1 & 0 \\ 0 & 0 & -1 \end{pmatrix}, \quad \Pi^2 = \mathbf{I}.
$$

A direct computation yields

$$
\Pi\mathbf{B}_i^{i+}\Pi = \mathbf{B}_i^{i-} \quad \text{for all } i,
$$

$$
\Pi\mathbf{B}_i^{1+}\Pi = -\mathbf{B}_i^{1-} \quad \text{for all } i \neq 1,
$$

$$
\Pi\mathbf{B}_3^{2+}\Pi = \mathbf{B}_3^{2-}.
$$

This implies that

$$
\Pi\mathbf{N}_+(\mu, \tilde{\xi})\Pi = \mathbf{N}_-(-\mu, \tilde{\xi}),
$$

for all $\mu \in \mathbb{C}$ and all $\tilde{\xi} \in \mathbb{R}^2$. Therefore, if $\mathbf{w} \in \ker(\mathbf{N}_+(\mu, \tilde{\xi}) + \lambda^2\mathbf{I})$ for some $\mu \in \mathbb{C}$, then $\Pi\mathbf{w} \in \ker(\mathbf{N}_-(-\mu, \tilde{\xi})) + \lambda^2\mathbf{I})$, and the stable modes μ_-^{s} at $\mathbf{F} = \underline{\mathbf{F}}^-$ can be computed from the unstable modes μ_+^{u} at the other well, by simply taking $\mu_-^{\mathrm{s}} = -\mu_+^{\mathrm{u}}$. Hence, it suffices to compute the unstable modes at $\mathbf{F} = \underline{\mathbf{F}}^+$. This symmetry provides a relation between the bundles $\hat{\mathbf{R}}$ as well. By direct computation one finds

$$
\Pi\mathbf{M}_{11}^+\Pi = -\mathbf{M}_{11}^-, \quad \Pi\mathbf{M}_{12}^+\Pi = \mathbf{M}_{11}^-,
$$

$$
\Pi\mathbf{M}_{22}^+\Pi = -\mathbf{M}_{22}^-, \quad \Pi\mathbf{M}_{21}^+\Pi = \mathbf{M}_{21}^-,
$$

and letting

$$
\Lambda := \begin{pmatrix} \Pi & 0 \\ 0 & -\Pi \end{pmatrix}, \quad \Lambda^2 = \mathbf{I},
$$

we arrive at the similarity condition

$$
\Lambda\mathbb{M}_+(\lambda, \tilde{\xi})\Lambda = -\mathbb{M}_-(\lambda, \tilde{\xi}), \tag{45}
$$

for all $(\lambda, \tilde{\xi}) \in \mathscr{S}$, which implies that if $\hat{\mathbf{R}}_+^{\mathrm{u}}$ is a continuous (analytic) representation on $\mathscr{S}^+$ of the unstable space of $\mathbb{M}_+(\lambda, \tilde{\xi})$, then the columns of

$$
\hat{\mathbf{R}}_-^{\mathrm{s}} := \Lambda\hat{\mathbf{R}}_+^{\mathrm{u}}, \tag{46}
$$

span the stable space of $\mathbb{M}_-(\lambda, \tilde{\xi})$ and constitute an analytic representation on $\mathscr{S}^+$ of this space (this follows by a simple dynamical systems argument). These bundles have continuous, full-rank extensions on the whole set $\mathscr{S}$. Consequently, it suffices to compute the unstable bundle $\hat{\mathbf{R}}_+^{\mathrm{u}}$. Notice also that $(0, \hat{e}_2^\top)\Lambda = (0, \hat{e}_2^\top)$, and that by Eq. (46), we have

$$
\hat{p}^+ = -\hat{p}^- = \varepsilon(0, \hat{e}_2^\top)\hat{\mathbf{R}}_+^{\mathrm{u}}.
$$

3.4. Using the homogeneity of Δ

From the definition of Δ, it is not hard to see that for all $\rho > 0$ and all $(\lambda, \tilde{\xi})$, there holds the homogeneity-like relation

$$\Delta(\lambda, \tilde{\xi}) = \Theta(\rho)\Delta(\rho\lambda, \rho\tilde{\xi}),$$

being Θ a continuous, non-vanishing factor, such that $|\Theta(\pm 1)| = 1$, $\Theta(\rho) \neq 0$. This property follows from the existence of a lifting matrix field $\mathscr{J}(\lambda, \tilde{\xi})$ with constant rank and linear in λ and $\tilde{\xi}$, which translates between original and reduced coordinates (Freistühler and Plaza, 2007). Without loss of generality we can assume $\tilde{\xi} \neq 0$ (see Appendix A). Therefore, we can normalize $(\lambda, \tilde{\xi}) \in \mathscr{S}$ by

$$\lambda \to \lambda/|\tilde{\xi}|, \quad \tilde{\xi} \to \tilde{\xi}/|\tilde{\xi}|,$$

and perform the computations on the set

$$|\tilde{\xi}| = 1, \quad \mathrm{Re}\,\lambda \geqslant 0, \quad \lambda \in \mathbb{C},$$

parametrizing $\tilde{\xi}$ in polar coordinates by

$$\tilde{\xi} = (\cos\varphi, \sin\varphi) = \mathrm{e}^{\mathrm{i}\varphi}, \quad \varphi \in [0, 2\pi).$$

Let us denote $\tilde{\mathbf{N}}_+(\mu, \varphi) := \mathbf{N}_+(\mu, \mathrm{e}^{\mathrm{i}\varphi})$. Since $\mathbf{N}_+(-\mu, -\tilde{\xi}) = \mathbf{N}_+(\mu, \tilde{\xi})$ for all μ and $\tilde{\xi}$, it suffices to take $\varphi \in [0, \pi]$. Finally, as $\tilde{\mathbf{N}}_+(-\mu, -\varphi) = \tilde{\mathbf{N}}_+(\mu, \varphi)$, we can restrict the computations to the quarter circle $\varphi \in [0, \frac{\pi}{2}]$, meaning no loss of generality. From this point on, we write indistinctively $\Delta(\lambda, \tilde{\xi})$ or $\Delta(\lambda, \varphi)$ to indicate $\Delta(\lambda, \mathrm{e}^{\mathrm{i}\varphi})$.

3.5. Summary

After these considerations, the stability function then takes the form

$$\Delta(\lambda, \tilde{\xi}) = \det\begin{pmatrix} \Lambda\hat{\mathbf{R}}_+^{\mathrm{u}} & \hat{Q} & \hat{\mathbf{R}}_+^{\mathrm{u}} \\ -\hat{p} & \hat{q} & \hat{p} \end{pmatrix}, \tag{47}$$

with

$$\begin{aligned}
\hat{Q} &= 2\varepsilon\begin{pmatrix} \hat{e}_2 \\ 0 \end{pmatrix} \in \mathbb{R}^{6\times 1}, \\
\hat{q} &= -\lambda(D_s h)_{|s=0} \in \mathbb{R}^{1\times 1}, \\
\hat{p} &= \varepsilon(0, \hat{e}_2^\top)\hat{\mathbf{R}}_+^{\mathrm{u}} \in \mathbb{C}^{1\times 3}, \\
\Lambda &= \mathrm{diag}(1, -1, -1, -1, 1, 1) \in \mathbb{R}^{6\times 6}, \tag{48}
\end{aligned}$$

for $(\lambda, \tilde{\xi})$ restricted to the set

$$\mathrm{Re}\,\lambda \geqslant 0, \quad \lambda \in \mathbb{C},$$

$$\tilde{\xi} = \mathrm{e}^{\mathrm{i}\varphi}, \quad \varphi \in [0, \pi/2].$$

4. Evaluating Δ

In this section we detail how to numerically evaluate the reduced Lopatinski function Δ associated to the martensite twin, in such a way that the numerical output provides secure information about the dynamical stability behaviour of the static interface.

4.1. Key ideas

4.1.1. The winding number argument

We will look at the family of mappings

$$\lambda \mapsto \bar{\Delta}(\cdot, \varphi), \quad \varphi \in [0, \pi/2],$$

for a suitable normalization of the stability function $\bar{\Delta}$ along the closed contours

$$\lambda \in \mathscr{C}_\rho := \mathscr{C}_\rho^+ \cup \mathscr{C}_\rho^0,$$

$$\mathscr{C}_\rho^+ := \{\lambda \in \mathbb{C} : |\lambda| = \rho, \operatorname{Re}\lambda > 0\},$$

$$\mathscr{C}_\rho^0 := \{\lambda \in \mathbb{C} : \lambda = i\tau, \tau \in [-\rho, +\rho]\},$$

for some $\rho > 0$ sufficiently large. Given that for $|\lambda| \gg 1$ large, $\Delta(\lambda, \tilde{\xi}) \sim \Delta(1, 0) \neq 0$ (see Appendix A below), the possible zeroes of $\bar{\Delta}$ are bounded in λ and it suffices to consider contours $\mathscr{C}_\rho$ with finite $\rho > 0$. By the product formula of mapping degrees (Deimling, 1985), the winding number of the curves $\lambda \mapsto \bar{\Delta}(\cdot, \varphi)$ with respect to zero determines the stability of the configuration.

4.1.2. The normalization

There is a major ambiguity in the definition (47), consisting in the freedom to choose specific representations $\hat{\mathbf{R}}_-^s$ of the stable space of $\mathbb{M}_-$, and $\hat{\mathbf{R}}_+^u$ of the unstable space of $\mathbb{M}_+$. This ambiguity can largely obscure the picture when one tries to apply the above computational evaluation of the winding number to the unmodified reduced Lopatinski function Δ. In fact, in order to proceed correctly in that direction, one would have to convince oneself that the concrete representations (chosen through formulation and computing methodology) are not only continuous along the curves $\mathscr{C}_\rho$, but can be extended, without modification, to continuous matrix functions of full rank at least on the whole interior of these curves. Given the fact, however, that they are three-dimensional sub-bundles of $\mathbb{C}^6$, there does not seem to exist an easy way of doing such verification. We completely circumvent this apparent difficulty by considering a normalized version of Δ,

$$\bar{\Delta} := \frac{\Delta}{-|\mathbf{R}|}, \tag{49}$$

with

$$|\mathbf{R}| := \det(\hat{\mathbf{R}}_-^s \hat{\mathbf{R}}_+^u) = \det(\Lambda \hat{\mathbf{R}}_+^u \hat{\mathbf{R}}_+^u). \tag{50}$$

The simple idea of this normalization is that it automatically undoes all possible extraneous winding. In other words: by whichever concrete factor the original Δ deviates from what it would be with respect to an admissible choice $\mathbf{R}_-^s, \mathbf{R}_+^u$ of the representation, the scaling denominator $|\mathbf{R}|$ deviates from the determinant $\det(\mathbf{R}_-^s \mathbf{R}_+^u)$ in exactly that way, and these two effects cancel each other out.

4.1.3. $\bar{\Delta}$ for Maxwell vs. Abeyaratne–Knowles kinetics

A simple consideration (see Section 4.4 below) on Δ and $|\mathbf{R}|$ shows that

$$\bar{\Delta} = \bar{\Delta}_0 - \lambda(D_s h), \tag{51}$$

where $\bar{\Delta}_0$ is the *normalized* Lopatinski function associated to Maxwell kinetics. This not only simplifies the algorithms considerably, but also gives a direct explanation of how the images of the curves $\mathscr{C}_\rho$ change upon going from vanishing to non-vanishing driving traction. We invite the reader to play with the geometric associations that formula (51) immediately prompts in that direction.

4.2. The Lopatinski modes

The essential piece in reliably determining the Lopatinski spaces is the identification of the frequencies. Once this is done in a secure way, standard algorithms allow to construct the bundle representation $\hat{\mathbf{R}}^u_+$ safely. We now discuss how to properly find the unstable μ-roots of

$$\pi_+(\mu) = \det(\mathbf{N}_+(\mu, \tilde{\xi}) + \lambda^2 \mathbf{I}) = \sum_{j=0}^{6} a_j \mu^j.$$

After cumbersome but straightforward computations, one finds that the coefficients $a_j = a_j(\lambda, \tilde{\xi}, \varepsilon)$ are given by

$$
\begin{aligned}
a_6 &= 2\varepsilon^6, \\
a_5 &= 0, \\
a_4 &= \lambda^2 \varepsilon^4 (2\varepsilon^2 + 5) + 6\varepsilon^6, \\
a_3 &= 2\varepsilon^5 \xi_2 \lambda, \\
a_2 &= 2\lambda^4 \varepsilon^3 (2 + \varepsilon^2) + \lambda^2 \varepsilon^4 ((10 + 3\varepsilon^2) + \varepsilon^2 \xi_3^2) + 6\varepsilon^6, \\
a_1 &= 2\lambda^2 \varepsilon^3 \xi_2 (\lambda^2 + \varepsilon^2), \\
a_0 &= \lambda^6 + \lambda^4 \varepsilon^2 (4 + \varepsilon^2) + \lambda^2 \varepsilon^4 ((5 + \varepsilon^2) + \varepsilon^2 \xi_3^2) + 2\varepsilon^6,
\end{aligned}
\tag{52}
$$

for each $(\lambda, \tilde{\xi}) \in \mathbb{C} \times \mathbb{R}^2$, with $|\tilde{\xi}| = 1$. Since $a_6 = 2\varepsilon^6 > 0$, we implemented a standard algorithm to compute the roots of the polynomial $\pi_+(\mu) = 0$. More precisely, we calculated the eigenvalues of

$$
\mathbf{G}(\lambda, \tilde{\xi}, \varepsilon) = \begin{pmatrix}
-a_5/a_6 & -a_4/a_6 & -a_3/a_6 & -a_2/a_6 & -a_1/a_6 & -a_0/a_6 \\
1 & 0 & 0 & 0 & 0 & 0 \\
0 & 1 & 0 & 0 & 0 & 0 \\
0 & 0 & 1 & 0 & 0 & 0 \\
0 & 0 & 0 & 1 & 0 & 0 \\
0 & 0 & 0 & 0 & 1 & 0
\end{pmatrix},
$$

via a standard Schur factorization for complex non-Hermitian matrices (Trefethen and Bau, 1997).

For values of λ with $\operatorname{Re}\lambda > 0$, the six μ-modes of $\pi_+(\mu) = 0$ are either stable or unstable. Fig. 2 shows the computed values of stable and unstable modes for $\lambda \in \mathscr{C}^+_\rho$, that is, along half circles, for different values of $\rho > 0$. They behave as unstable/stable in trios, with neutral limits as $\operatorname{Re}\lambda \to 0^+$.

For values of λ along the imaginary axis, neutral modes can occur. These neutral modes, however, are the continuous limits of stable or unstable modes as $\operatorname{Re}\lambda \to 0^+$. When a neutral mode μ is the limit of a stable (resp. unstable) mode we call it *neutrally stable* (resp. *neutrally unstable*). Therefore, the roots of π_+ come always in trios of stable/neutrally stable or unstable/neutrally unstable modes.

We designed a direct algorithm to determine the stability nature of the neutral modes along the imaginary axis, using a simple perturbation method. For each $\lambda = i\tau \in i\mathbb{R}$ we make $\tilde{\lambda} = i\tau + \delta$ with small $\delta > 0$ and compute the perturbed eigenmodes. Estimating the minimum distance between the latter and the original neutral mode, we select the associated stable or unstable mode which, by continuity, tends to the original neutral μ as $\delta \to 0^+$. In the case of coalescence, that is, when there is a multiple neutral mode, the algorithm safely keeps track of the perturbed modes already selected, in such a way that it produces exactly three stable/ neutrally stable and three unstable/neutrally unstable values, respecting the hyperbolic dichotomy (it can happen that a multiple neutral mode is at the same time the limit of stable and unstable modes). In our computations we take δ of order $\mathcal{O}(10^{-6})$.
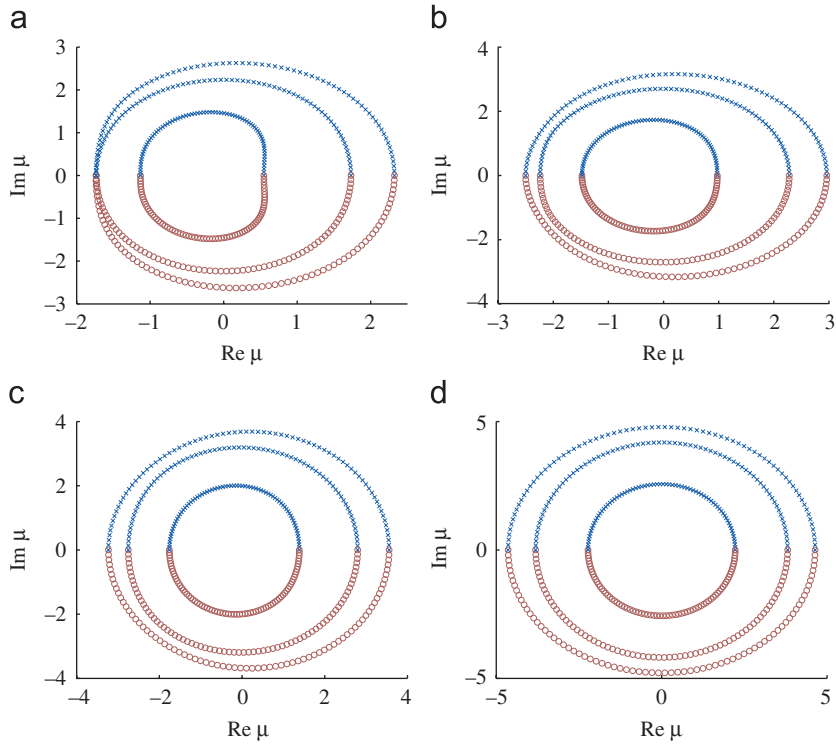
Fig. 2. Computed values of the eigenmodes μ for $(\lambda, \tilde{\xi}) = (\rho e^{i\theta}, e^{i\varphi})$, $\theta \in [0, \pi]$, for parameter values of (a) $(\rho, \varphi) = (1, 0)$, (b) $(\rho, \varphi) = (5/4, \pi/8)$, (c) $(\rho, \varphi) = (3/2, \pi/4)$, and (d) $(\rho, \varphi) = (2, \pi/2)$. The unstable modes μ^u with $\operatorname{Im} \mu > 0$ are depicted with blue crosses, whereas the stable modes μ^s with $\operatorname{Im} \mu < 0$ are represented by circles in red. The x- and y-axes correspond to the real and imaginary parts of μ, respectively. Notice that the (continuous) eigenmodes come in trios of stable and unstable ones, depicted in the figure as three curves in the upper and lower half planes. The eigenmodes approach the real line only when λ approaches the imaginary axis, that is, when $\theta = 0$ or $\theta = \pi/2$. In these cases, they are called neutrally stable or neutrally unstable, depending on whether they are the limit of strictly stable or strictly unstable eigenmodes, respectively. In all computations we set the material parameter as $\varepsilon = 0.5$.

For values of λ along the imaginary axis we expect the presence of *branch points*, for example, values of τ for which the eigenmodes μ change from neutral to stable/unstable, or points where two or more modes coalesce. Fig. 3 shows computed values of the unstable modes along an interesting portion of the imaginary axis, namely, near zero (for τ large the modes are always neutral), and for different values of φ. We observe that the modes coalesce, for instance, at $\lambda = 0$. To illustrate the phenomenon of neutral to stable/unstable branching, Fig. 4 depicts the imaginary parts of the unstable modes μ^u against $\tau \in [-1, 1]$, again, for different values of φ. The existence of six branch points of real-to-complex type is clear.

4.3. Evaluation of the bundle $\hat{\mathbf{R}}^u_+$

Once the Lopatinski frequencies have been computed, we proceed to assemble the unstable Lopatinski bundle $\hat{\mathbf{R}}^u_+$ according to formula (43). The main step is the computation of the kernel of $\tilde{\mathbf{N}}_+(\mu^u_j, \varphi) + \lambda^2 \mathbf{I}$, where μ^u_j is the unstable mode under consideration. For that purpose, we use a simple cross-product algorithm that calculates $\mathbf{w}_j$ in Eq. (44) and numerically verifies the result for each unstable/neutrally unstable mode μ^u_j. Following Eq. (43), we assemble the unstable bundle by taking

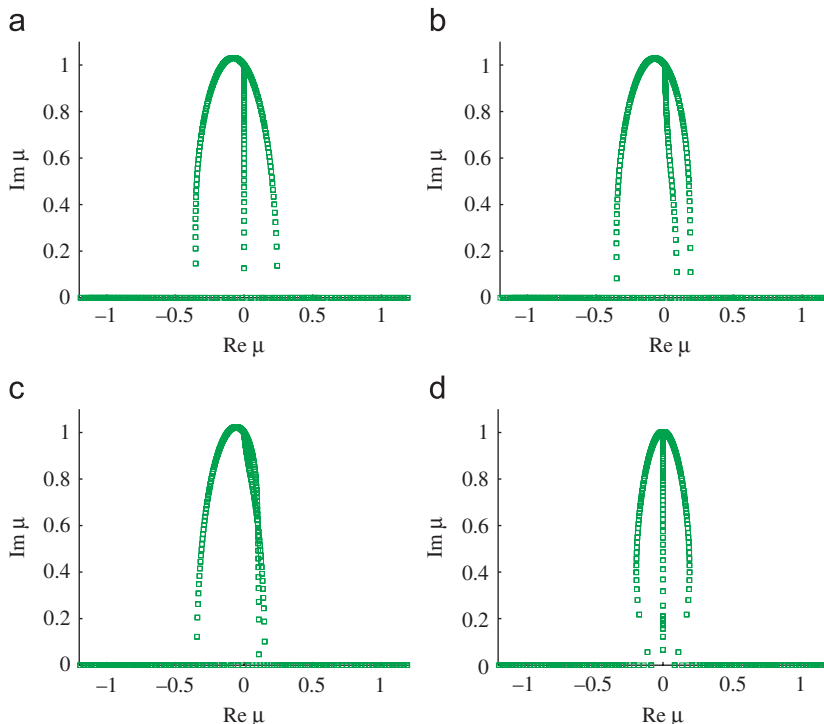$$\hat{\mathbf{R}}^u_+ = (\mathbf{r}_1 \ \ \mathbf{r}_2 \ \ \mathbf{r}_3),$$

Fig. 3. Computed values of the unstable eigenmodes μ^{u} for $(\lambda, \tilde{\xi}) = (i\tau, e^{i\varphi})$, $\tau \in [-1, 1]$, and for different values of (a) $\varphi = 0$, (b) $\varphi = \pi/8$, (c) $\varphi = \pi/4$, and (d) $\varphi = \pi/2$. The *x*- and *y*-axes correspond to real and imaginary parts of μ^{u}, respectively. Notice that along $\lambda \in i\mathbb{R}$ there exist neutral modes with $\mathrm{Im}\,\mu = 0$. In particular, all the modes are neutral for $|\tau|$ large. Also note that some of the eigenmodes coalesce for certain values of τ. In all computations we set the material parameter as $\varepsilon = 0.5$.

where each column is given by

$$\mathbf{r}_j = \begin{pmatrix} \mathbf{w}_j \\ i(\mu_j^{\mathrm{u}} \mathbf{B}_1^{1\pm} + \xi_2 \mathbf{B}_2^{1\pm} + \xi_3 \mathbf{B}_3^{1\pm})\mathbf{w}_j \end{pmatrix}, \quad j = 1, 2, 3.$$

At most points, the constructed bundle is a valid, full-rank representation of the unstable Lopatinski space, with the exception of a discrete set of branch points associated to multiple modes where non-trivial Jordan blocks may occur. This factor, however, appears at the same order in both the numerator and the denominator of Eq. (49), cancelling each other out, and yields the desired effect of the normalization

4.4. Reduction of determinants

Finally, one can make further reductions on the expression for $\bar{\Delta}$ in order to arrive at formula (51). Suppose $\hat{\mathbf{R}}_+^{\mathrm{u}}$ is a continuous representation of the unstable space of $\mathbb{M}_+$. Let us define

$$\hat{\mathbf{R}}_+^{\mathrm{u}} =: \begin{pmatrix} \mathbf{y}_1 \\ \mathbf{y}_2 \\ \mathbf{y}_3 \\ \mathbf{z}_1 \\ \mathbf{z}_2 \\ \mathbf{z}_3 \end{pmatrix}, \tag{53}$$

so that

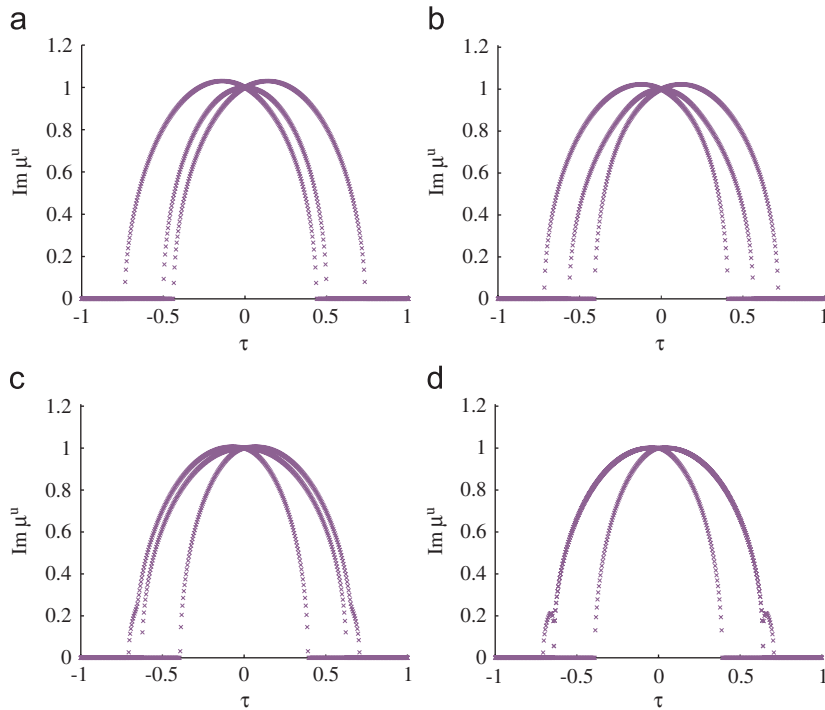$$\mathbf{y}_j, \mathbf{z}_j : \mathscr{S} \longrightarrow \mathbb{C}^{1 \times 3},$$

Fig. 4. Values of the imaginary parts of the unstable modes μ^{u} for $(\lambda, \tilde{\xi}) = (i\tau, e^{i\varphi})$ (that is, for λ along the imaginary axis), plotted versus $\tau \in [-1, 1]$ for parameter values of (a) $\varphi = 0$, (b) $\varphi = \pi/4$, (c) $\varphi = 4\pi/9$, and (d) $\varphi = \pi/2$. Observe the branching phenomenon in which the unstable modes become neutral at a certain point τ_*. From the figure we can identify six of these branch points of neutral-to-stable type, of the form $\lambda_j = \pm i\tau_j$, $j = 1, 2, 3$, with $0 < \tau_1 < \tau_2 < \tau_3 < 1$. Since the order of the characteristic polynomial is 6, these are the only branching points, all located in this portion of the imaginary axis near zero, and all the modes remain neutral for $|\tau|$ large enough. Like before, in all computations we set the material parameter as $\varepsilon = 0.5$.

are three-dimensional *row* vector-valued functions of $(\lambda, \tilde{\xi})$. From Eqs. (47) and (48), the reduced Lopatinski function takes the form

$$
\Delta = \begin{vmatrix}
\mathbf{y}_1 & 0 & \mathbf{y}_1 \\
-\mathbf{y}_2 & 2\varepsilon & \mathbf{y}_2 \\
-\mathbf{y}_3 & 0 & \mathbf{y}_3 \\
-\mathbf{z}_1 & 0 & \mathbf{z}_1 \\
\mathbf{z}_2 & 0 & \mathbf{z}_2 \\
\mathbf{z}_3 & 0 & \mathbf{z}_3 \\
-\varepsilon\mathbf{z}_2 & -\lambda(D_s h) & \varepsilon\mathbf{z}_2
\end{vmatrix}.
$$

Performing elementary column–row transformations and pivoting on the middle column, we obtain

$$
\Delta = 8 \begin{vmatrix}
\mathbf{y}_1 & 0 & \mathbf{y}_1 \\
\mathbf{z}_2 & 0 & \mathbf{z}_2 \\
\mathbf{z}_3 & 0 & \mathbf{z}_3 \\
0 & 0 & \mathbf{y}_3 \\
0 & 0 & \mathbf{z}_1 \\
0 & 2\varepsilon & \mathbf{y}_2 \\
0 & -\lambda(D_s h) & \varepsilon\mathbf{z}_2
\end{vmatrix}
= 16\varepsilon \begin{vmatrix}
\mathbf{y}_1 & \mathbf{y}_1 \\
\mathbf{z}_2 & \mathbf{z}_2 \\
\mathbf{z}_3 & \mathbf{z}_3 \\
0 & \mathbf{y}_3 \\
0 & \mathbf{z}_1 \\
0 & \varepsilon\mathbf{z}_2
\end{vmatrix}
+ 8\lambda(D_s h) \begin{vmatrix}
\mathbf{y}_1 & \mathbf{y}_1 \\
\mathbf{z}_2 & \mathbf{z}_2 \\
\mathbf{z}_3 & \mathbf{z}_3 \\
0 & \mathbf{y}_3 \\
0 & \mathbf{z}_1 \\
0 & \mathbf{y}_2
\end{vmatrix}
$$

$$= 16\varepsilon^2 \begin{vmatrix} \mathbf{y}_1 \\ \mathbf{z}_2 \\ \mathbf{z}_3 \end{vmatrix} \begin{vmatrix} \mathbf{y}_3 \\ \mathbf{z}_1 \\ \mathbf{z}_2 \end{vmatrix} + 8\lambda(D_s h) \begin{vmatrix} \mathbf{y}_1 \\ \mathbf{z}_2 \\ \mathbf{z}_3 \end{vmatrix} \begin{vmatrix} \mathbf{y}_3 \\ \mathbf{z}_1 \\ \mathbf{y}_2 \end{vmatrix} = 8\Gamma_{(0)}(2\varepsilon^2 \Gamma_{(1)} + \lambda(D_s h)\Gamma_{(2)}), \tag{54}$$

where

$$\Gamma_{(0)}(\lambda, \tilde{\xi}) := \begin{vmatrix} \mathbf{y}_1 \\ \mathbf{z}_2 \\ \mathbf{z}_3 \end{vmatrix}, \quad \Gamma_{(1)}(\lambda, \tilde{\xi}) := \begin{vmatrix} \mathbf{y}_3 \\ \mathbf{z}_1 \\ \mathbf{z}_2 \end{vmatrix}, \quad \Gamma_{(2)}(\lambda, \tilde{\xi}) := \begin{vmatrix} \mathbf{y}_3 \\ \mathbf{z}_1 \\ \mathbf{y}_2 \end{vmatrix}. \tag{55}$$

Similarly, from the definition (50) of $|\mathbf{R}|$, we have

$$|\mathbf{R}| = \begin{vmatrix} \mathbf{y}_1 & \mathbf{y}_1 \\ -\mathbf{y}_2 & \mathbf{y}_2 \\ -\mathbf{y}_3 & \mathbf{y}_3 \\ -\mathbf{z}_1 & \mathbf{z}_1 \\ \mathbf{z}_2 & \mathbf{z}_2 \\ \mathbf{z}_3 & \mathbf{z}_3 \end{vmatrix} = 8 \begin{vmatrix} \mathbf{y}_1 & \mathbf{y}_1 \\ \mathbf{z}_2 & \mathbf{z}_2 \\ \mathbf{z}_3 & \mathbf{z}_3 \\ 0 & \mathbf{z}_1 \\ 0 & \mathbf{y}_2 \\ 0 & \mathbf{y}_3 \end{vmatrix} = 8 \begin{vmatrix} \mathbf{y}_1 \\ \mathbf{z}_2 \\ \mathbf{z}_3 \end{vmatrix} \begin{vmatrix} \mathbf{z}_1 \\ \mathbf{y}_2 \\ \mathbf{y}_3 \end{vmatrix} = 8\Gamma_{(0)}\Gamma_{(2)}.$$

In view of the normalization (49), this finally implies that
$$\bar{\Delta} = \bar{\Delta}_0 - \lambda(D_s h), \tag{56}$$

where

$$\bar{\Delta}_0 = -2\varepsilon^2 \frac{\begin{vmatrix} \mathbf{y}_3 \\ \mathbf{z}_1 \\ \mathbf{z}_2 \end{vmatrix}}{\begin{vmatrix} \mathbf{z}_1 \\ \mathbf{y}_2 \\ \mathbf{y}_3 \end{vmatrix}} = -2\varepsilon^2 \frac{\Gamma_{(1)}}{\Gamma_{(2)}} \tag{57}$$

is the *normalized* Lopatinski function associated to Maxwellian kinetics.

Thus, all we need to do is safely compute the bundle $\hat{\mathbf{R}}_+^u$, rearrange its entries in the two 3×3 determinants $\Gamma_{(1)}$ and $\Gamma_{(2)}$, and evaluate their quotient (57).

5. Output and stability results

This section displays the results of our computations, in which we fixed the value of the material parameter as $\varepsilon = 0.5$. In what follows we reckon kinetic relations of *linear* type, as proposed originally by Abeyaratne and Knowles (1990) for irreversible processes close to thermodynamic equilibrium. These have the form

$$\mathscr{F} = \frac{s}{M}, \tag{58}$$

where $M > 0$ is a *mobility coefficient*; or, in other words,

$$h = -\frac{s}{M}, \tag{59}$$

and

$$D_s g = D_s(\mathscr{F} + h) = -\frac{1}{M}.$$

Clearly, when $M \to +\infty$ we recover the Maxwell rule.

We computed the parametrized curves $\lambda \mapsto \bar{\Delta}(\cdot, \varphi)$, $\lambda \in \mathscr{C}_\rho$, with finite $\rho > 0$ and for different parameter values of φ, under both the Maxwell rule and linear kinetic rules with different values of $M > 0$. Since $\bar{\Delta}$ is

continuous in $\varphi \in [0, \pi/2]$, we chose $\varphi = 0, \pi/8, \pi/4, 3\pi/8$, and $\pi/2$ in order to illustrate the continuous behaviour along the whole parameter set, as snapshots of a curve in motion. In each of the figures presented in the following pages, the blue dots correspond to values of $\bar{\Delta}$ for $\lambda = i\tau$ with $\tau > 0$, whereas the red circles represent values of $\bar{\Delta}$ for $\lambda = i\tau$ with $\tau < 0$; the green dots correspond to the values of $\bar{\Delta}$ for $\lambda \in \mathscr{C}_\rho^+$. Each figure shows a detailed view of an interesting part of the imaginary axis (left), say $i\tau \in i[-1, 1]$, and of the whole contour $\mathscr{C}_\rho$ (right). The x- and y-axes correspond to values of $\operatorname{Re}\bar{\Delta}$ and $\operatorname{Im}\bar{\Delta}$, respectively.

5.1. Maxwell kinetic rule: $M = +\infty$

Our first calculation considered Maxwellian kinetics. Figs. 5 show the computed curves $\lambda \mapsto \bar{\Delta}_0(\cdot, \varphi)$, $\lambda \in \mathscr{C}_\rho$, with $\rho = 1.5$, corresponding to vanishing driving traction. We set the parameter values as (a) $\varphi = 0$, (b) $\varphi = \pi/8$, (c) $\varphi = \pi/4$, (d) $\varphi = 3\pi/8$, and (e) $\varphi = \pi/2$. For instance, in Fig. 5(a) for $\varphi = 0$, we notice the presence of two zeroes of $\bar{\Delta}_0$ of form $\lambda = \pm i\tau_0$ for some $\tau_0 > 0$, as the curve passes through zero twice, once for $\lambda = +i\tau_0$ (blue dot), and once for its symmetric $\lambda = -i\tau_0$ (red circle). By continuity of the Lopatinski function in φ, this behaviour persists for $\varphi > 0$ small. Again, since the curves are like snapshots of a curve in motion parametrized by φ, we notice, in Fig. 5(b) for $\varphi = \pi/8$, that the curve touches the real axis at positive values of $\bar{\Delta}_0$, but no zeroes along the imaginary axis occur. This suggests, by continuity, that for a critical value φ_c with $0 < \varphi_c < \pi/8$, the curves pass from having two zeroes of form $(\lambda, \xi) = (\pm i\tau_\varphi, e^{i\varphi})$ for all $0 \leqslant \varphi < \varphi_c$, a situation which corresponds to a "cone" of double zeroes (cone in the $\tilde{\xi} = e^{i\varphi}$ variable) along the imaginary axis, to having none for $\varphi_c < \varphi < \pi/2$, as can be observed from Figs. 5(c) and (d).

Observe in Fig. 5(e), however, the presence of two isolated zeroes at $\lambda = \pm i\tau_*$ for $\varphi = \pi/2$ and some $\tau_* > 0$. They are isolated because if we perform the calculations for values of φ approaching $\pi/2$ from below, the behaviour illustrated by Fig. 5(d), for which there are no zeroes of form $(\lambda, \xi) = (\pm i\tau, e^{i\varphi})$, persists along the parameter values $3\pi/8 < \varphi < \pi/2$ by continuity. In the limit $\varphi = \pi/2$, the two zeroes occur as can be observed in Fig. 5(e). If we allow the parameter value φ to move beyond $\varphi > \pi/2$, then the previous behaviour for $\varphi < \pi/2$ occurs by symmetry, and the zeroes must be isolated. Finally, notice that by a winding number argument, there are no zeroes inside the contour (with $\operatorname{Re}\lambda > 0$) for all values of φ under consideration. The only zeroes found along the imaginary axis are of form $(\pm i\tau_\varphi, e^{i\varphi})$ for all $0 \leqslant \varphi < \varphi_c < \pi/8$, and the isolated zeroes $(\pm i\tau_*, e^{i\pi/2})$, suggesting the existence of *surface waves*. These observations imply *weak stability* of the twin for Maxwellian kinetics.

5.2. Linear kinetic rules with $0 < M < +\infty$

If we substitute the Maxwell rule by linear kinetic functions as described above, and take bounded, positive values of the mobility coefficient M, we observe a stabilizing effect. We computed the curves $\lambda \mapsto \bar{\Delta}(\cdot, \varphi)$, for $\lambda \in \mathscr{C}_\rho$ with $\rho = 1.5$, substituting $D_s h = -1/M$ in formula (51) for different values of M. Figs. 6, 7, and 8 show the computed curves for values of $M = 100$, $M = 10$, and $M = 1$, respectively, and for parameter values of (a) $\varphi = 0$, (b) $\varphi = \pi/8$, (c) $\varphi = \pi/4$, (d) $\varphi = 3\pi/8$, and (e) $\varphi = \pi/2$. In contrast to what happens for Maxwellian kinetics, we observe now that the main geometrical property of the curves is precisely that zero remains outside the contour, showing the evanescence of the winding number of the curves with respect to zero, for *all* parameter values of φ. Notice that for λ along the imaginary axis, $\lambda = i\tau$, with small values of τ, the curves show an "opening" which avoids the real axis, and the values of $\bar{\Delta}$ along this segment have a non-zero imaginary part (except at $\lambda = 0$), as suggested intuitively by formula (51). This behaviour can be observed in all Figs. 6(a)–(e) on the left, depicting the curves for λ along a segment of the imaginary axis. When we decrease the mobility coefficient, this "opening" of the curves avoiding the real axis is even more accentuated and visible, as we can observe from Figs. 7(a)–(e) and 8(a)–(e). Notice that the winding number of each of these closed curves with respect to zero is zero, showing the non-evanescence of the stability function inside and along the whole contour. These observations and the arguments given above indicate that the twin is *uniformly stable* with respect to linear kinetic rules of Abeyaratne and Knowles type.
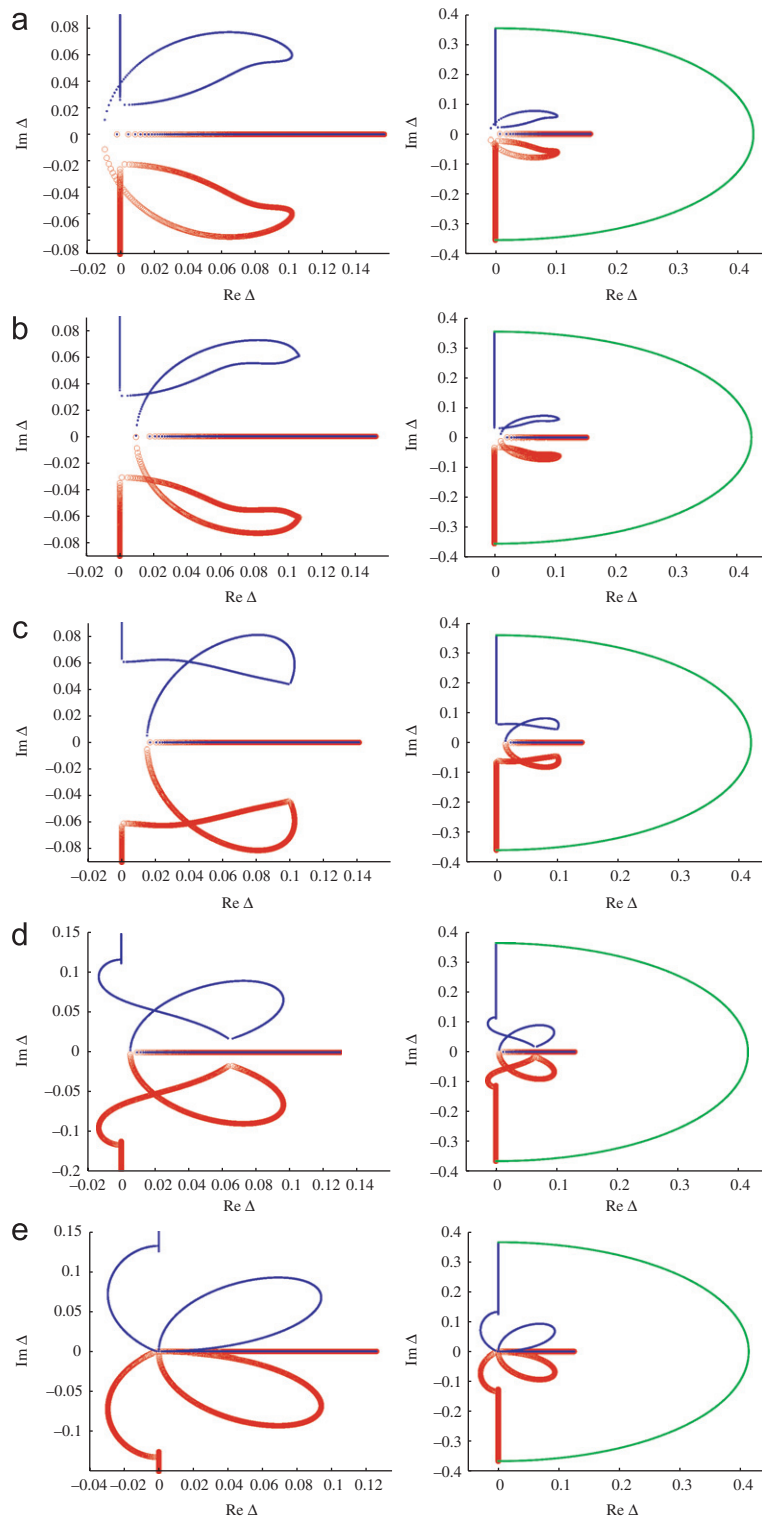
Fig. 5. *Maxwell kinetic rule*: Images of the curves $\lambda \mapsto \bar{\Delta}_0(\cdot, \varphi)$ with $M = +\infty$, for values of λ along a portion of the imaginary axis (left), and the whole contour $\mathscr{C}_\rho$ (right) with $\rho = 1.5$. The graphs correspond to parameter values of (a) $\varphi = 0$, (b) $\varphi = \pi/8$, (c) $\varphi = \pi/4$, (d) $\varphi = 3\pi/8$, and (e) $\varphi = \pi/2$.
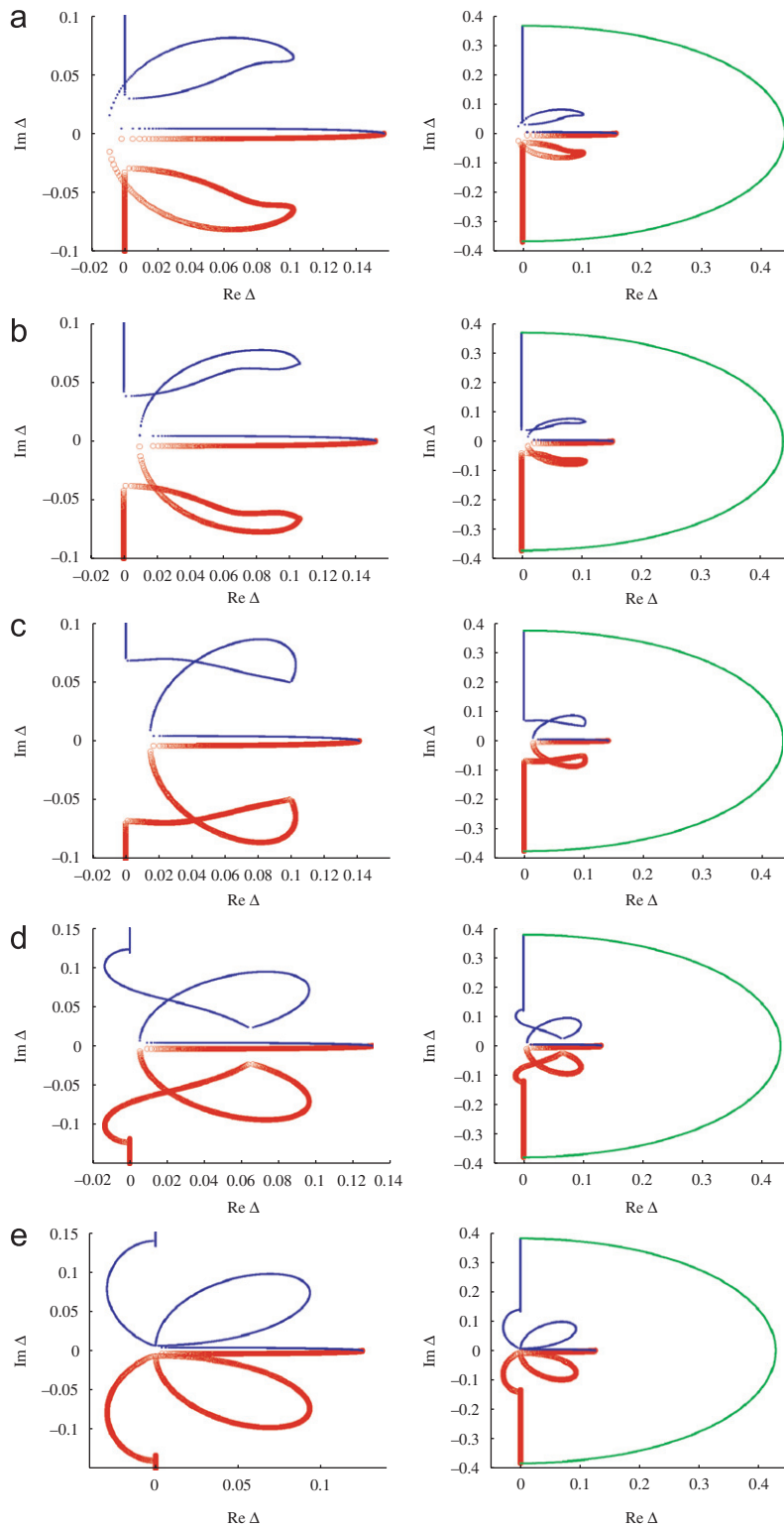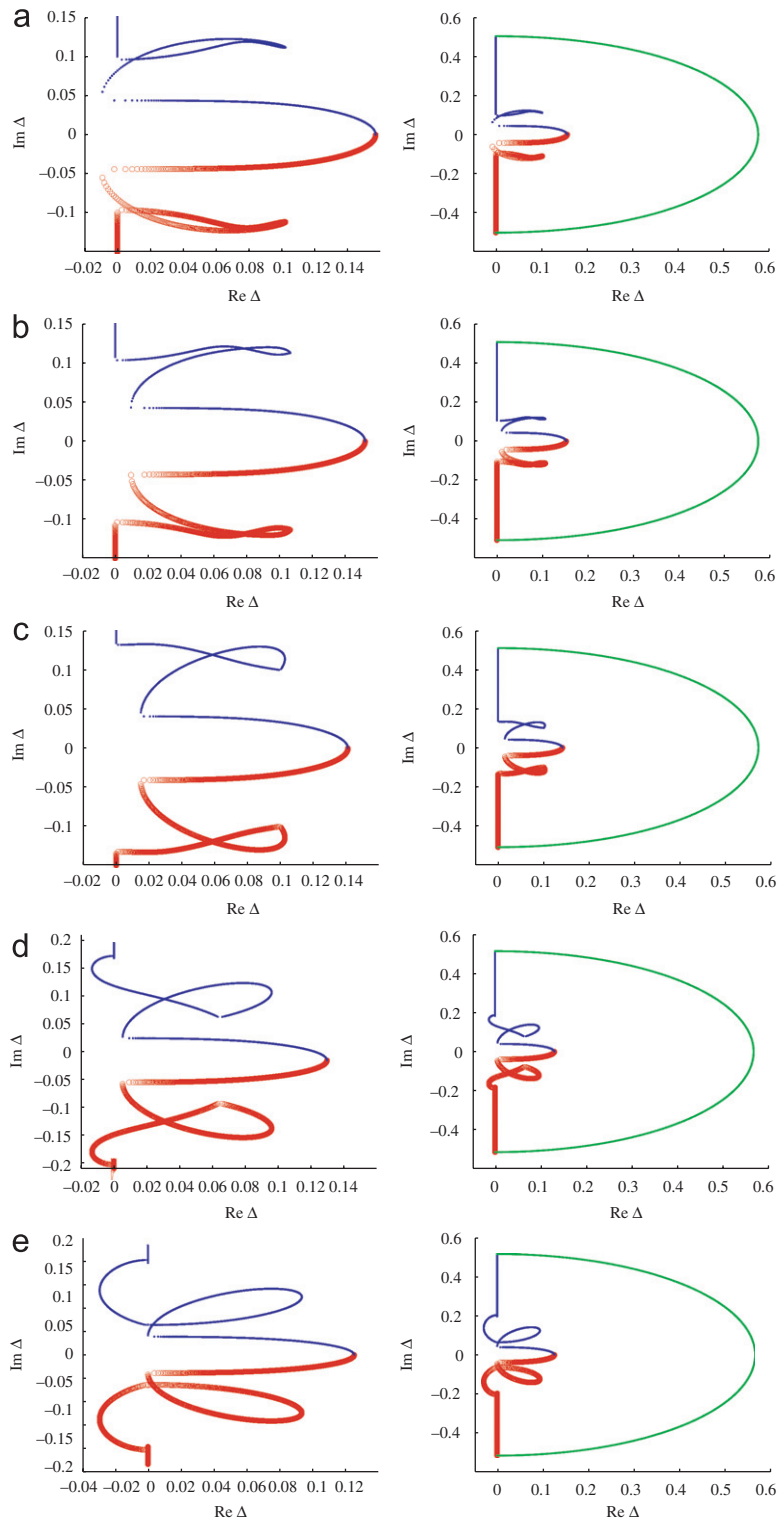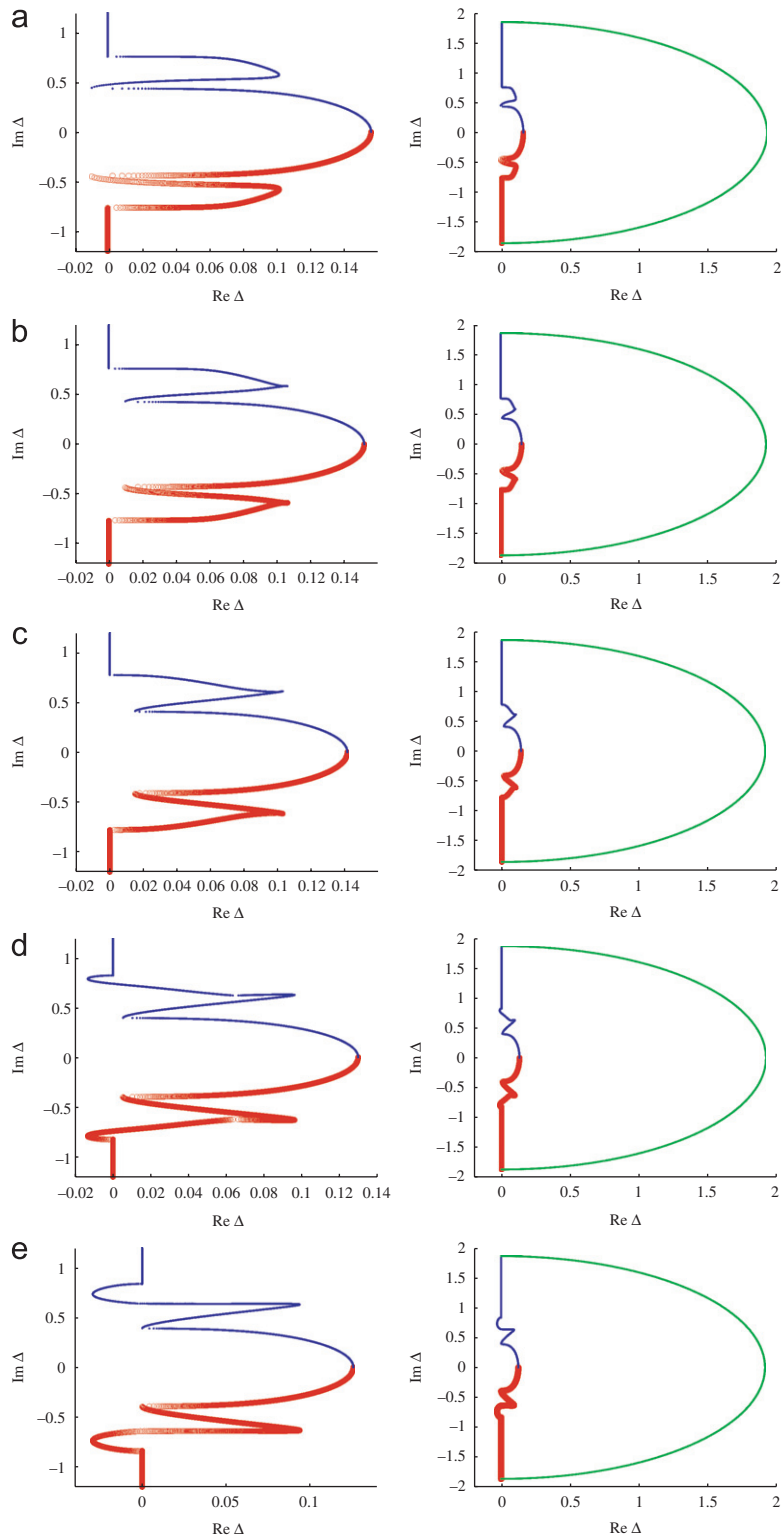
Fig. 6. *Linear kinetic rule with $M = 100$*: Images of the curves $\lambda \mapsto \bar{\Delta}(\cdot, \varphi)$ with $M = 100$, for values of λ along a portion of the imaginary axis (left), and the whole contour $\mathscr{C}_\rho$ (right) with $\rho = 1.5$. The graphs correspond to parameter values of (a) $\varphi = 0$, (b) $\varphi = \pi/8$, (c) $\varphi = \pi/4$, (d) $\varphi = 3\pi/8$, and (e) $\varphi = \pi/2$.

Fig. 7. *Linear kinetic rule with $M = 10$:* Images of the curves $\lambda \mapsto \bar{\Delta}(\cdot, \varphi)$ with $M = 10$, for values of λ along a portion of the imaginary axis (left), and the whole contour $\mathscr{C}_\rho$ (right) with $\rho = 1.5$. The graphs correspond to values of (a) $\varphi = 0$, (b) $\varphi = \pi/8$, (c) $\varphi = \pi/4$, (d) $\varphi = 3\pi/8$, and (e) $\varphi = \pi/2$.

Fig. 8. *Linear kinetic rule with M = 1*: Images of the curves $\lambda \mapsto \bar{\Delta}(\cdot, \varphi)$ with $M = 1$, for values of λ along a portion of the imaginary axis (left), and the whole contour $\mathscr{C}_\rho$ (right) with $\rho = 1.5$. The graphs correspond to values of (a) $\varphi = 0$, (b) $\varphi = \pi/8$, (c) $\varphi = \pi/4$, (d) $\varphi = 3\pi/8$, and (e) $\varphi = \pi/2$.

5.3. Numerical extrapolation of the limit $M \to 0^+$

We may ask about the behaviour of the curves when the mobility M goes to zero in Eq. (58). Although taking the limit to zero mobility in *linear* rules like Eq. (58) may seem artificial (it means that not even an infinite force is able to make the boundary move), the result corresponds to an effective relation for a ''pinned'' boundary, in which small imperfections of the material lead to a macroscopic kinetic relation characterized by zero mobility at least along a portion near the origin in the $\mathscr{F}$-axis (see, e.g., Abeyaratne et al., 1996; Bhattacharya, 1999). By performing the numerical computation of $\bar{\Delta}$ for small values of M, one observes that the curves have a limiting behaviour, and that they do not change much its form (modulo some scaling) when $M \to 0^+$. To illustrate this, Figs. 9 depict the computed curves $\lambda \mapsto \Delta(\cdot, \varphi)$, for $\lambda \in \mathscr{C}_\rho$ with $\rho = 1$, when the mobility coefficient is set to $M = 1 \times 10^{-4}$. As before, the figures correspond to values of (a) $\varphi = 0$, (b) $\varphi = \pi/8$, (c) $\varphi = \pi/4$, (d) $\varphi = 3\pi/8$, and (e) $\varphi = \pi/2$, showing the curves for λ along a portion of the imaginary axis on the left, and along the whole contour, on the right. Of course, the diameter of the closed contours blow up in size proportionally to $1/M$. The images on the right seem to show that the curves pass through zero due to the scales; but detailed pictures near zero on the left prove that this is not the case. We observe, then, the same stable behaviour as for mobilities bounded below, in which the winding numbers of the curves with respect to zero vanish, as expected. Similar (almost identical up to scaling) pictures of the curves can be numerically obtained for values $M = 1 \times 10^{-5}$ and 1×10^{-6}.

6. Discussion

1. In this work, we presented a direct procedure to compute numerically the stability function associated to a well known example of a martensite twin. Thanks to analiticity/continuity properties of the stability function and by a winding number argument, our computations show that the twin is weakly stable under the Maxwell kinetic rule (conservation of energy across the interface), whereas it is uniformly stable under dissipative kinetic rules of linear type proposed by Abeyaratne and Knowles (1990). Our numerical results seem to be the elastic counterpart to the analytic results of Benzoni-Gavage (1998, 1999) in the case of two-phase fluid flow. This study pertains to the stability of a specific elastic martensite twin towards fully three-dimensional perturbations, and it is the first of its kind, up to our knowledge.

2. We have numerically located certain zeroes of the stability function along the imaginary axis in the case when the interface and its perturbations are subject to the Maxwell kinetic rule. Just like in the case of phase boundaries for van der Waals fluids governed by Maxwelliam kinetics (Benzoni-Gavage, 1998), this fact refers to the possible existence of *surface waves*. The latter are non-trivial solutions of form (19) with $(\lambda, \breve{\xi}) = (\mathrm{i}\tau, \breve{\xi})$, points where $\bar{\Delta}$ vanishes, and with $(\hat{\mathbf{F}}^\pm, \hat{\mathbf{v}}^\pm)(+\infty) = 0$. The amplitudes $(\hat{\mathbf{F}}^\pm, \hat{\mathbf{v}}^\pm)(\cdot)$ are exponentially decreasing at $+\infty$ and the waves are then localized near the interface (hence the name surface waves). The existence and precise description of such waves are topics that still have to be investigated.

3. Our analysis and computational methodology may serve as a blueprint to study other energy densities under different regular kinetic models of particular interest. Positive stability results in these other contexts may be taken as a criterion for the modelling of phase-boundary dynamics in real materials, in the sense that a regular kinetic relation which does not pass a simple multidimensional stability test can hardly be accepted to describe stably moving planar interfaces.

4. In this work, we selected kinetic relations in their simplest form, describing irreversible processes close to equilibrium (Abeyaratne and Knowles, 1990, 1991). They express the driving force across the interface as a function of the boundary speed. More complex theories prescribe kinetic relations depending, in addition, on interfacial stress and energy (Gurtin and Struthers, 1990), or on interfacial orientation (Rosakis and Tsai, 1995). It is not yet clear what are the effects of such kinetics on multidimensional stability.

5. Notice that the kinetic rules of linear type (58) express the driving force as a *monotonic* function of the phase-boundary speed. The class of kinetic rules defined by Eqs. 18(a)–(d) is, however, more general. For instance, non-monotonic kinetic relations have been proposed before in the literature (see, e.g., Rosakis and Knowles, 1997). Concerning predictions for *regular* non-monotonic kinetic relations in the particular
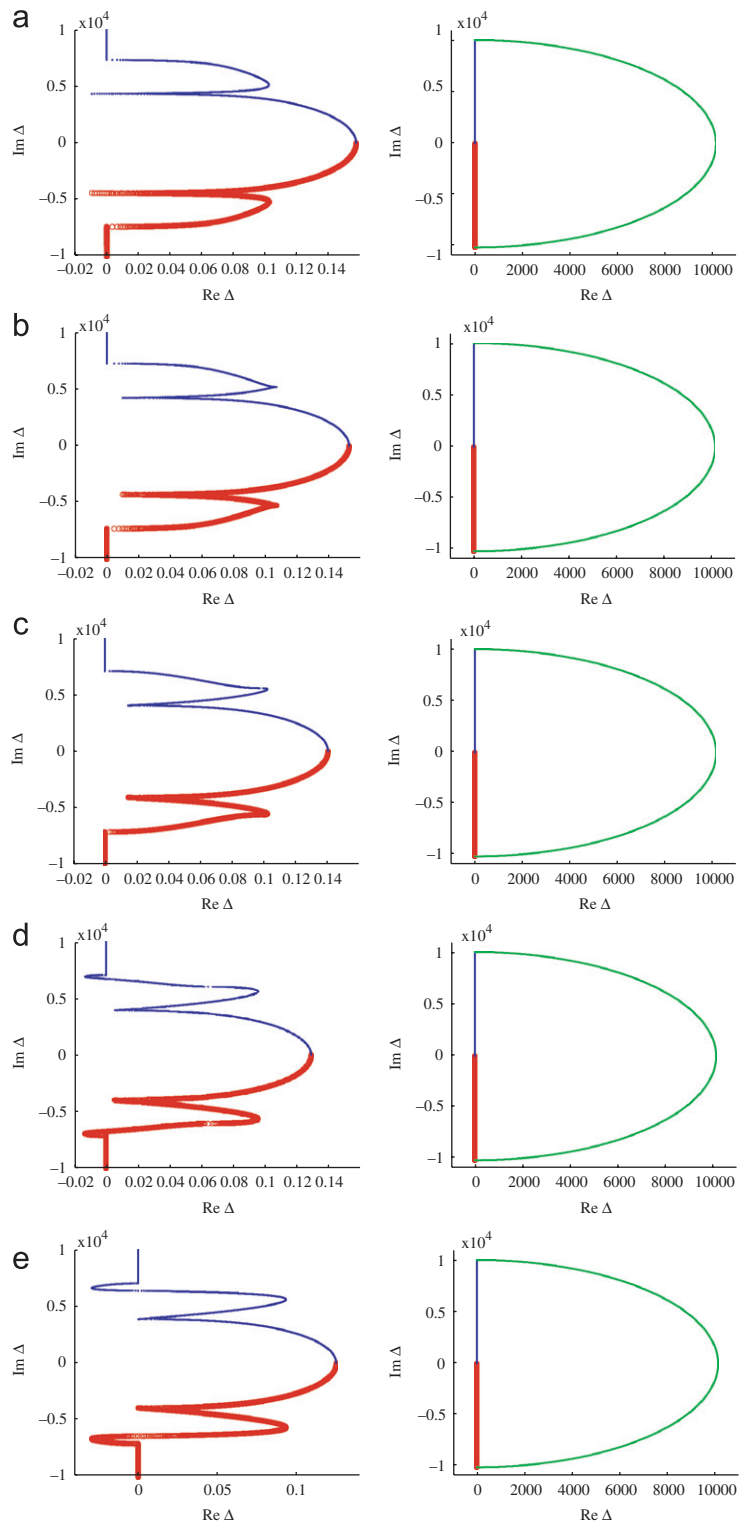
Fig. 9. *Numerical extrapolation of the limit $M \to 0^+$: Images of the curves $\lambda \mapsto \bar{\Delta}(\cdot, \varphi)$ with $M = 1 \times 10^{-4}$, for values of λ along a portion of the imaginary axis (left), and the whole contour $\mathscr{C}_\rho$ (right) with $\rho = 1$. The graphs correspond to values of (a) $\varphi = 0$, (b) $\varphi = \pi/8$, (c) $\varphi = \pi/4$, (d) $\varphi = 3\pi/8$, and (e) $\varphi = \pi/2$.*

case of *static* martensite twins, we conjecture that our observations on stability (weak stability under Eqs. 18(a)–(c) versus uniform stability under Eqs. 18(a)–(d)) remain valid, as long as the kinetic rule is monotonic in a neighborhood of $s = 0$, as suggested by Eq. 18(d) and formula (51). The consequences of non-monotonicity of regular kinetic rules on multidimensional stability of more general *moving* boundaries are not yet fully understood.

6. We emphasize that the definition and solution theory of the stability function applies only to *regular* kinetic rules which are, at least, once differentiable on its parameters. Our results and methodology do not take into account discontinuous kinetic functions, or with discontinuous derivatives, which abound in the literature as phenomenological models like lattice trapping or maximally dissipative processes (see, e.g., Abeyaratne and Knowles, 2006), to mention just a few. The multidimensional stability of phase boundaries under non-regular kinetic relations is an important topic of further investigation.

Acknowledgements

Appendix A. One-dimensional stability: $\Delta(\lambda, 0) \neq 0$

In this appendix we include the computation of $\Delta(\lambda, 0)$ which can be seen as a one-dimensional stability analysis. This is a straightforward calculation as the spectral analysis of $\mathbb{M}_+$ reduces to that of $\mathbf{B}_1^{1\pm}$. Make $\tilde{\xi} = 0$ with $(\lambda, 0) \in \mathscr{S}$. The unstable eigenvalues of $\mathbb{M}_+(\lambda, 0)$ are

$$\mu_j = +\frac{i\lambda}{\sqrt{k_j}}, \quad j = 1, 2, 3,$$

where k_j are the real, positive, and distinct eigenvalues (28) of $\mathbf{B}_1^{1\pm}$. A simple computation shows that the corresponding eigenvectors are

$$\mathbf{w}_2 = \hat{e}_3, \quad \mathbf{w}_j = k_j \begin{pmatrix} 2\varepsilon^3 \\ k_j - 2\varepsilon^2 \\ 0 \end{pmatrix}, \quad j = 1, 3.$$

Following formula (43), the unstable bundle of $\mathbb{M}_+(\lambda, 0)$ takes the (full rank) form

$$\hat{\mathbf{R}}_+^u(\lambda, 0) = \begin{pmatrix} \mathbf{w}_1 & \mathbf{w}_2 & \mathbf{w}_3 \\ i\mu_1 k_1 \mathbf{w}_1 & i\mu_2 k_2 \mathbf{w}_2 & i\mu_3 k_3 \mathbf{w}_3 \end{pmatrix},$$

so that, in the notation of Section 4.4,

$$\mathbf{y}_1 = 2\varepsilon^3(k_1, 0, k_3),$$
$$\mathbf{y}_2 = (k_1(k_1 - 2\varepsilon^2), 0, k_3(k_3 - 2\varepsilon^2)),$$
$$\mathbf{y}_3 = (0, 1, 0),$$
$$\mathbf{z}_1 = -2\lambda\varepsilon^3(k_1\sqrt{k_1}, 0, k_3\sqrt{k_3}),$$
$$\mathbf{z}_2 = -\lambda(k_1\sqrt{k_1}(k_1 - 2\varepsilon^2), 0, k_3\sqrt{k_3}(k_3 - 2\varepsilon^2)),$$
$$\mathbf{z}_3 = -\lambda\varepsilon(0, 1, 0).$$

We compute the determinants (55),

$$\Gamma_{(0)}(\lambda, 0) = 2\lambda^2 \varepsilon^6 \sqrt{k_1} \sqrt{k_3} (\sqrt{k_1} - \sqrt{k_3})((1 + 2\varepsilon^2)\sqrt{k_1}\sqrt{k_3} + 2\varepsilon^2) \neq 0,$$

$$\Gamma_{(1)}(\lambda, 0) = 4\lambda^2 \varepsilon^7 \sqrt{k_1} \sqrt{k_3}(k_1 - k_3) \neq 0,$$

$$\Gamma_{(2)}(\lambda, 0) = 2\lambda \varepsilon^3 k_1 k_3 (\sqrt{k_3} - \sqrt{k_1})(2\varepsilon^2 + \sqrt{k_1}\sqrt{k_3}) \neq 0,$$

which are all non-vanishing for $(\lambda, 0) \in \mathcal{S}$, as the eigenvalues satisfy $0 < k_1 < k_2 < k_3$. Thus, we obtain for the Maxwell rule that

$$\Delta_0 = 16\varepsilon^2 \Gamma_{(0)} \Gamma_{(1)} \sim C\lambda^4 \neq 0.$$

For regular Abeyaratne–Knowles rules (with $(D_s h) < 0$) we get

$$\Delta = 8\Gamma_{(0)}(2\varepsilon^2 \Gamma_{(1)} + \lambda(D_s h)\Gamma_{(2)})$$
$$= 16\Gamma_{(0)}\lambda^2 \varepsilon^3 (\sqrt{k_1} - \sqrt{k_3})(4\varepsilon^6 \sqrt{k_1}\sqrt{k_3}(\sqrt{k_1} + \sqrt{k_3}) - (D_s h)k_1 k_3(2\varepsilon^2 + \sqrt{k_1}\sqrt{k_3}))$$
$$\sim C\lambda^4 \neq 0.$$

Hence,

$$\Delta(\lambda, 0) \neq 0, \quad \mathrm{Re}\,\lambda \geqslant 0, \quad |\lambda| = 1,$$

for both Maxwell and regular Abeyaratne–Knowles kinetic rules.

References

Abeyaratne, R., Knowles, J.K., 1990. On the driving traction acting on a surface of strain discontinuity in a continuum. J. Mech. Phys. Solids 38 (3), 345–360.

Abeyaratne, R., Knowles, J.K., 1991. Kinetic relations and the propagation of phase boundaries in solids. Arch. Ration. Mech. Anal. 114, 119–154.

Abeyaratne, R., Knowles, J.K., 2006. Evolution of Phase Transitions: A Continuum Theory. Cambridge University Press, Cambridge.

Abeyaratne, R., Chu, D., James, R.D., 1996. Kinetics of materials with wiggly energies: theory and application to the evolution of twinning microstructures in a Cu–Al–Ni shape memory alloy. Philos. Mag. A 73 (2), 457–497.

Ball, J.M., James, R.D., 1987. Fine phase mixtures as minimizers of energy. Arch. Ration. Mech. Anal. 100 (1), 13–52.

Ball, J.M., James, R.D., 1992. Proposed experimental tests of a theory of fine microstructure and the two-well problem. Philos. Trans. R. Soc. London Ser. A 338, 389–450.

Benzoni-Gavage, S., 1998. Stability of multi-dimensional phase transitions in a van der Waals fluid. Nonlinear Anal. TMA 31 (1–2), 243–263.

Benzoni-Gavage, S., 1999. Stability of subsonic planar phase boundaries in a van der Waals fluid. Arch. Ration. Mech. Anal. 150, 23–55.

Bhattacharya, K., 1999. Phase boundary propagation in an heterogeneous body. R. Soc. Lond. Proc. Ser. A Math. Phys. Eng. Sci. 455, 757–766.

Ciarlet, P.G., 1988. Mathematical elasticity. Vol. I: three-dimensional elasticity. In: Studies in Mathematics and its Applications, vol. 20. North-Holland Publishing Co., Amsterdam.

Coulombel, J.-F., 2003. Stability of multidimensional undercompressive shock waves. Interfaces Free Bound 5 (4), 360–390.

Dafermos, C., 2005. Hyperbolic Conservation Laws in Continuum Physics, second ed. Springer, Berlin.

Deimling, K., 1985. Nonlinear Functional Analysis. Springer, Berlin.

Ericksen, J.L., 1975. Equilibrium of bars. J. Elasticity 5 (3–4), 191–201.

Freistühler, H., 1995. A short note on the persistence of ideal shock waves. Arch. Math. 64, 344–352.

Freistühler, H., 1998. Some results on the stability of non-classical shock waves. J. Partial Diff. Equations 11 (1), 25–38.

Freistühler, H., Plaza, R.G., 2007. Normal modes and nonlinear stability behaviour of dynamic phase boundaries in elastic materials. Arch. Ration. Mech. Anal. 186 (1), 1–24.

Gurtin, M.E., Struthers, A., 1990. Multphase thermomechanics with interfacial structure III: evolving phase boundaries in the presence of bulk deformation. Arch. Ration. Mech. Anal. 112 (2), 97–160.

Hersh, R., 1963. Mixed problems in several variables. J. Math. Mech. 12 (3), 317–334.

James, R.D., 1980. The propagation of phase boundaries in elastic bars. Arch. Ration. Mech. Anal. 73 (2), 125–158.

Kreiss, H.O., 1970. Initial boundary value problems for hyperbolic systems. Commun. Pure Appl. Math. 23, 277–298.

Kružík, M., Luskin, M., 2003. The computation of martensitic microstructures with piecewise laminates. J. Sci. Comput. 19 (1–3), 293–308.

Lax, P.D., 1957. Hyperbolic systems of conservation laws II. Commun. Pure Appl. Math. (10), 537–566.

Majda, A., 1983a. The stability of multi-dimensional shock fronts. Mem. Am. Math. Soc. 41 (275), iv + 95.

R.G. Plaza / J. Mech. Phys. Solids 56 (2008) 1989–2018

Majda, A., 1983b. The existence of multi-dimensional shock fronts. Mem. Am. Math. Soc. 43 (281), v + 93.

Métivier, G., 1990. Stability of multidimensional weak shocks. Commun. Partial Diff. Equations 15 (7), 983–1028.

Métivier, G., 2000. The block structure condition for symmetric hyperbolic systems. Bull. London Math. Soc. 32 (6), 689–702.

Rosakis, P., Knowles, J.K., 1997. Unstable kinetic relations and the dynamics of solid–solid phase transitions. J. Mech. Phys. Solids 45 (11–12), 2055–2081.

Rosakis, P., Tsai, H., 1995. Dynamic twinning processes in crystals. Int. J. Solids Struct. 32 (17–18), 2711–2723.

Trefethen, L.N., Bau III, D., 1997. Numerical Linear Algebra. Society for Industrial and Applied Mathematics (SIAM), Philadelphia, PA.